ADJUSTMENT FACTORS FOR MEPDG PAVEMENT RESPONSES CONSIDERING THREE-DIMENSIONAL ANALYSIS AND WIDE-BASE TIRE

BY

OSMAN ERMAN GUNGOR

THESIS

Submitted in partial fulfillment of the requirements
for the degree of Master of Science in Civil Engineering
in the Graduate College of the
University of Illinois at Urbana-Champaign, 2015

Urbana, Illinois

Adviser:

Professor Imad L. Al-Qadi

ABSTRACT

The Mechanistic-Empirical Pavement Design Guide (MEPDG) provides a superior methodology as compared to its predecessor in the design and analysis of pavement structures. The mechanistic (MEDPG analysis) calculates critical pavement responses due to pavement-tire interactions. On the other hand, the empirical part refers to the prediction of pavement distress propagation over time using transfer functions. Transfer functions link critical pavement responses to particular pavement distresses. Although MEPDG analysis provides a theoretically framework for pavement simulations, its limitations and simplifications may produce inaccurate pavement response calculations. In contrast, finite element (FE) analysis has proven capable of overcoming these limitations by simulating pavement more realistically in terms of material characterization and loading conditions. However, the high computational cost of the FE analysis precludes its use as a pavement analysis engine within the MEPDG's framework. Therefore, this study suggests two adjustment factors based on FE analysis to bridge the gap between reality and MEPDG analysis. The first adjustment factor—developed utilizing 480 cases performed in ABAQUS and considering similar material properties and pavement structure—converts pavement responses obtained from dual tire assembly (DTA) loading to new generation wide base tire (NG-WBT) loading. The second adjustment factor—developed from running 336 cases in MEPDG and FE analyses using compatible input parameters—accounts for the limitations of MEPDG analysis regarding the material characterization and loading conditions. The simulated cases were selected to capture extreme conditions—e.g., thick and thin pavement structures with strong and weak material properties—so that extrapolation could be avoided during the implementation of the equations. The adjustment factors revealed that NG-WBT produces higher responses than DTA, which can cause greater pavement damage. Additionally, MEPDG analysis fails to capture the effect of non-uniformity and the three dimensionality of contact stress on pavement response. The discrepancy becomes significant; especially for the pavement responses near the pavement surface, such as tensile strain at the AC surface and vertical shear strain within the AC layer, that are believed to cause top-down cracking.

To Father, Mother and Brother

ACKNOWLEDGEMENTS

First and foremost, I would like to express my gratitude to Professor Imad Al-Qadi for his support and guidance during this process of study. I would also like to thank him for his valuable advice regarding my personal and academic career.

I want to thank Dr. Hasan Ozer for his unlimited support throughout my master's program. He has always had time, answers, and advice for problems, both personal and professional.

I would also like to thank all my friends in Chambana and ATREL who made my stay a memorable one. I specifically thank my dear friend Ozan Kahraman for his consistent support.

Finally, I owe my deepest gratitude to my family: my father Teoman Gungor, my mother Bircan Gungor, and my older brother Cenk Gungor. They have provided constant support throughout my life, and I have always felt extremely lucky to have such a wonderful family.

TABLE OF CONTENTS

LIST OF TABLES

LIST OF FIGURES

CHAPTER 1

INTRODUCTION

1.1 Motivation and Background

According to the American Society of Civil Engineering (ASCE), the United States has four million miles of highway pavement, which has been deteriorating rapidly due to increasing passenger and freight traffic demand. ASCE states that the federal, state and local agencies spend $91 billion annually to maintain and rehabilitate highways in the U.S. (2013 Report card, 2013).

One of the approaches to reduce this very high cost is to accurately predict pavement performance over time. Numerous studies have thus sought to understand the behavior of pavement under tire loading in order to develop more reliable pavement design and analysis methods. The AASHO Road test, started in 1958, was the first attempt to develop a methodology for pavement design that resulted in AASHTO 1961, 1972, 1986 and 1993 Pavement Design guides. Significant changes in pavement design inputs became available since the inaugural AASHO road test.

In 1998, the NCHRP 1-37A was launched to develop a new pavement and analysis method guide capable of incorporating developments in material characterization and vehicular loading, and to consider direct climate effects on pavement behavior. After six years of research, the Mechanistic-Empirical Pavement Design Guide (MEPDG) was released in 2004. The mechanistic part of the MEPDG simulates the pavement-tire interaction to compute critical pavement responses. The empirical part of the MEPDG links calculated critical pavement responses to corresponding pavement distress and predicts pavement deterioration over time using transfer functions.

The mechanistic part of the MEPDG analysis provides a framework for pavement response to vehicular loading. It recognizes the fact that asphalt concrete (AC) exhibits viscoelastic behavior and considers the effects of aging, temperature, and loading frequency. However, simplifications and limitations in the method may produce inaccurate pavement response calculations. The linear elastic analysis of AC and base materials, spring model assumption for layer interface, vertical uniform tire pressure, and circular contact area all represent limitations of MEPDG analysis. In addition to producing inaccurate pavement response calculations for dual-tire assembly (DTA)

loading, these shortcomings also preclude MEPDG's ability to simulate wide base tire (WBT) loading.

1.2 Objective and Research Approach

The objective of this study is to mend the gap between reality and MEPDG analysis by modifying the MEPDG analysis pavement responses in accordance with finite element (FE) analysis. Finite element analysis has proven a promising numerical method that can overcome MEPDG analysis limitations; however, it is computationally costly to be used as a pavement analysis engine in MEPDG. The proposed modifications will enable MEPDG to consider WBT loading and complexities in pavement behavior without implement FE analysis.

The research approach is to divide MEPDG limitations into two sets and develop an adjustment factor for each. The first set relates to the inability of MEPDG to simulate WBT loading. The second set of limitations pertains to complexities in pavement simulation that are not considered in MEPDG, such as 3-D non-uniform contact stresses, explicit viscoelastic characterization of AC, and non-linear stress-dependent characterization of granular material. The approach is demonstrated in Figure 1.

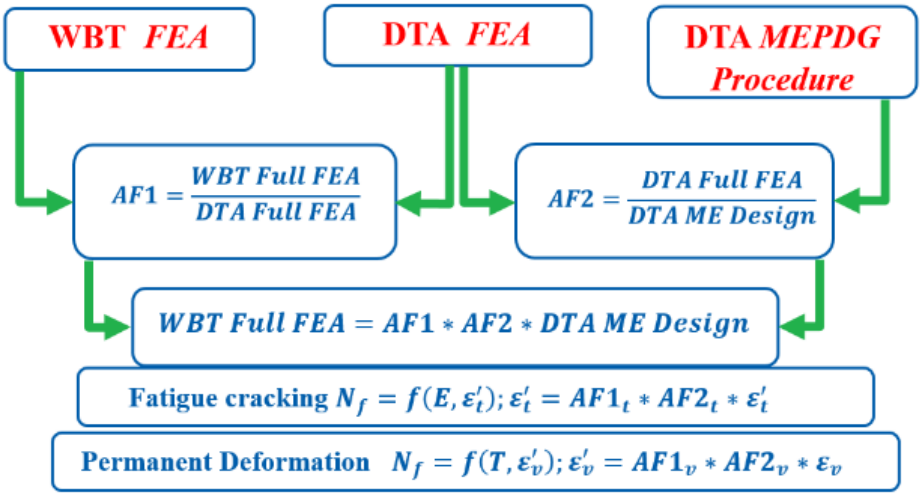

Figure 1: Adjustment factor development and application approach

1.3 Scope

In the following chapter, Chapter Two, presents adjustment factor 1 (DTA to NG-WBT) along with the three dimensional FE model of pavement. Chapter Three provides an explanation of the development of adjustment factor 2 (MEPDG analysis to FE analysis). MEPDG analysis and its limitations are also explained in detail. Finally, Chapter Four presents the conclusions of this study and suggests future research directions.

1.4 Impact of the Study

Accurate prediction of pavement performance plays a key role in developing effective pavement design options and maintenance strategies. The MEPDG is a state-of-art methodology for designing and rehabilitating pavement structure. However, it does not simulate NG-WBT loading and overlooks a number of realistic conditions for pavement-tire interaction. This study assists MEPDG to obtain more accurate pavement responses. This also allows accurate prediction of pavement damage and hence, the associated costs, which in turn, results in the help in better allocation of needed funds for pavement construction and rehabilitation.

CHAPTER 2

QUANTITATIVE ASSESSMENT OF THE EFFECT OF WIDE-BASE TIRES ON PAVEMENT RESPONSE USING FINITE ELEMENT ANALYSIS

Various studies in the literature have shown that the new generation wide-base tire (NG-WBT) causes more damage to pavement than dual-tire assembly (DTA). However, there is no substantive approach that quantifies the difference in pavement responses produced by NG-WBT and DTA. The study presented in this chapter fills this gap by developing linear equations that connect pavement responses produced by these two different tire types. The equations are developed for ten different pavement responses using 480 finite element method (FEM) simulations (240 for DTA and 240 for NG-WBT), which were run in ABAQUS considering the same material properties and pavement structures. The only difference was the contact stresses and contact areas which were measured under the same axle load for NG-WBT and DTA. The cases modelled in simulations were selected in a way to capture extreme conditions, i.e., thick and thin pavement structures with strong and weak material properties. The equations developed will help pavement researchers to quantitatively understand the effect of NG-WBT on pavement responses compared to DTA. The low resultant prediction error, 10%, allows linear equations to be implemented through applying adjustment factors on mechanistic pavement design guides like the Mechanistic–Empirical Pavement Design Guide (MEPDG), which are unable to simulate NG-WBT loading realistically. To accurately predict pavement damage, the pavement analysis should consider the NG-WBT market penetration in the US (approximately 10%) and the partial use of NG-WBT on truck axles. The impact of NG-WBT on pavement should be evaluated in the context of its economic and environmental benefits.

2.1 Introduction

According to a 2013 Environmental Protection Agency report, 27% of greenhouse gas (GHG) emission was produced by the transportation sector (U.S. Greenhouse Gas, 2014). This makes transportation the second highest source of GHG after electricity production (31%). Therefore, many attempts have been made in the last decade to reduce the environmental impact of the transportation sector. Replacing conventional dual tires with NG-WBT is one such development related to pavement engineering in the transportation sector.

Wide-base tires were introduced to market in early 1980s and have been extensively used especially in Europe and Canada. Improving fuel efficiency, providing better handling and breaking, and reducing gross weight, emission, tire replacement, and maintenance cost are some reported benefits of using NG-WBT (Ang-Olson et al., 2002; Al-Qadi et al.,2015; Wang et al., 2010). On the other hand, even though trucks equipped with wide-base tires can be safely approached to the side of the road under a blown-out tire event, a safety issue associated with the failure of wide-base tires has also been reported. Unlike DTA, no other tire helps the driver to reach the next service station in case of a blown out wide-base tire.

The main concern about the wide-base tire, however, has been raised by state and federal transportation agencies concerning the pavement damage caused by NG-WBT compared with DTA. There has been a number of studies that investigated the effect of NG-WBT on pavement performance. Most of these studies have agreed on the fact that NG-WBT generally causes more damage to the pavement than DTA. However, none of those studies quantifies the difference in pavement responses generated by NG-WBT vs. DTA.

This study fills this gap by presenting linear equations that connect pavement responses produced by these two different tire types. The equations have been developed for ten different pavement responses using a total of 480 finite element method (FEM) simulations, which were run in ABAQUS considering the same material properties and pavement structures. The cases simulated in ABAQUS were selected in a way to capture extreme conditions, i.e., thick and thin pavement structures with strong and weak material properties. The tire types considered in the simulations are NG-WBT 445/50 R22.5 and DTA 275/80 R22.5, which are the most commonly used in the market. The equations developed provide pavement researchers with a more comprehensive insight into the effect of NG-WBT on pavement behavior. Additionally, this study provides pavement design guides like Mechanistic-Empirical Pavement Design Guide (MEPDG) with the opportunity to consider NG-WBT loading without having to implement advanced structural analysis methods like FEM.

2.2 Background

Among the major efforts made in the transportation sector to reduce the sector's environmental impact is the replacement of DTA with NG-WBT. NG-WBT introduces several advantages, such as reducing fuel cost and improving breaking and handling. However, pavement researchers and engineers raised a concern that WBT may cause a higher damage to pavement compared with DTA since it has a smaller contact area. Therefore, a large number of studies has been conducted to investigate the effect of WBT on pavement structure. These studies can be classified into two groups: studies conducted between 1980s and 2000, which consider that WBT causes higher damage to pavement than DTA and which led tire industries to produce the so-called "new-generation" WBT (NG-WBT) with a wider tread than its predecessors; and studies investigating NG-WBT. Following is a summary of the studies conducted to estimate the damage effects of first-generation and NG-WBT.

In 1986 and 1989, Huhtala and his coworkers. (Huhtala, 1986; Huhtala at al., 1989) presented two studies using accelerated pavement testing on three different pavement sections with various loading conditions. Comparison of these two tire types was done based on the pavement response of tensile strain at the bottom of asphalt concrete (AC) and vertical pressure at the top of the subgrade. They concluded that WBT causes approximately 4 times more damage to pavement than DTA. Similar conclusions were reported by Sebaaly et al in 1989 (Sebaaly et al., 1989) who found that WBT results in 50 % greater tensile strain at the bottom of AC and 25% greater compressive stress with HMA compared with dual tires. Akram et al. (Akram et al., 1992) used multidepth deflectometers (MDDs) to quantify the damage effects of DTA versus WBT. Two different pavement structure types were considered in the experiments: thin and thick pavements. It was reported that WBT produces 2.5 times and 2.8 time more rutting damage on thick and thin pavements, respectively. Similarly, Bonaquist et al. (Bonaquist et al., 1992) stated that WBT produces 2 times more permanent deformation and causes 25% less fatigue life than DTA.

The NG-WBT with wider tread was introduced to the market at the beginning of the 2000s. In 2001, experimental studies were conducted in Europe to investigate the effect of NG-WBT on pavement responses (Faber et al., 2000). Two different pavement sections were built in the United Kingdom to compare NG-WBT (495/45R22.5) with traditional NG-WBT (385/65R22.5). This study found out that the traditional NG-WBT-385 causes 50% and 70% more rutting damage to

medium-thick and thin flexible pavement, respectively. The effect of NG-WBT on thick pavement was evaluated in Germany where NG-WBT was compared with a DTA; it was reported that NG-WBT causes 30% more rutting damage compared with DTA. Another comparison between DTA and NG-WBT was conducted in France on very thick and stiff pavement. This study showed that there is no significant difference between these two types of tires for this type of pavement. An extensive test matrix was performed in Virginia including 12 different pavement sections, two different axle loads, and four different tire pressures (Al-Qadi et al., 2004; Al-Qadi et al., 2005). Comparing NG-WBT with DTA, it was found that the former type of tires is, in general, less damaging. Two NG-WBT tires, NG-WBT-425 and NG-WBT-455, and DTA were compared to investigate their effects on full-depth pavement at the University of Illinois at Urbana-Champaign (Al-Qadi et al., 2009; Wang et al., 2009). NG-WBT-425 was found to be more damaging than NG-WBT-455.

Most studies have come to the conclusion that both first-generation WBT and NG-WBT cause more pavement damage than DTA. However, most of these conclusions have been derived based on a limited number of pavement structures, loading cases, and material characterization. Experimental evaluation of pavement performance is not only time consuming but also expensive and cumbersome. Therefore, none of the past studies has proposed a general mathematical relationship connecting these two tire types in terms of pavement behavior. The study presented in this chapter fills this gap in the literature by proposing linear equations that convert the pavement responses obtained from DTA to NG-WBT. Finite element (FE) analysis was used to develop the equations. Using FE analysis in this study gave the advantage of considering a wide variety of cases for pavement structure, material properties, and loading conditions that would not be feasible in any experimental study.

2.3. 3-D Finite Element Model

Simulating flexible pavement is a challenging task. Other than its geometry, every component of the simulation, such as the loading conditions and material characterization, is complicated. The tire applies non-uniform and three-dimensional contact stresses on the pavement. Asphalt material exhibits viscoelastic behavior, meaning that its behavior depends on time (aging), temperature, and frequency of loading. Stiffness of the granular material depends on the stress level at which it is being exposed. While granular material shows stiffer behavior under a high stress level, it gets

softer when the stress is low. Moreover, the material behaves differently in each principal direction, i.e., it is considered an anisotropic material. The literature clarifies the significant effect of these conditions on pavement responses (Al-Qadi et al., 2008; Siddharthan et al., 1998; Yoo et al., 2006). Therefore, it is important to capture them while simulating pavement behavior under the tire load to compute the pavement responses accurately.

The linear elastic theory (LET) is the current analysis approach used in mechanistic-empirical design guides. However, it fails to simulate pavement-tire interaction realistically because of its inability to adopt some of the abovementioned conditions. Linear elastic characterization of asphalt concrete and base materials, spring model assumption for layer interface, vertical uniform tire pressure, and circular contact area are only some examples of the unrealistic simplifications and assumptions of LET. Besides the fact that these assumptions may lead to inaccurate pavement response calculation for DTA loading, dividing axle load by tire pressure is not the realistic representation of NG-WBT contact area.

The FE method, on the other hand, has proved to be a promising numerical method which could successfully simulate loading conditions and account for non-linearity in material characterization. Therefore, the FEM has gained popularity over the last decade. The pavement FE model presented in this paper is the ultimate version of over ten years of on-going research (Wang et al., 2010;,Yoo et al., 2006; Elseifi et al., 2006; Yoo et al., 2007; Al-Qadi et al., 2007). It is capable of considering the conditions omitted by LET. Moreover, the developed model has been successfully validated using experimental field data from various pavement sections (Gungor et al., In Review). The key features of the developed FE model can be categorized into five different groups: model geometry and boundary conditions, loading conditions, material characterization, analysis method, and interface interaction model. A brief explanation for each key feature is given in the following sections.

2.3.1 Model Geometry and Boundary Conditions

The FEM of flexible pavement structure that was developed in commercial FE software, ABAQUS v 6.13, is given in Figure 2. It is known that FEM generates more accurate results as the size of the element gets smaller; but it is computationally expensive. Therefore, mesh sensitivity analysis was performed to optimize accuracy and computation time. In order to perform mesh sensitivity

analysis, an elastic FE model was compared to an LET software, BISAR, for six different critical pavement responses: maximum transverse and longitudinal tensile strain at the bottom of AC; maximum compressive strain within subgrade; and maximum vertical shear strain within AC, base, and subgrade. The model was refined until the difference in the results between the FE model and BISAR was around 5%.

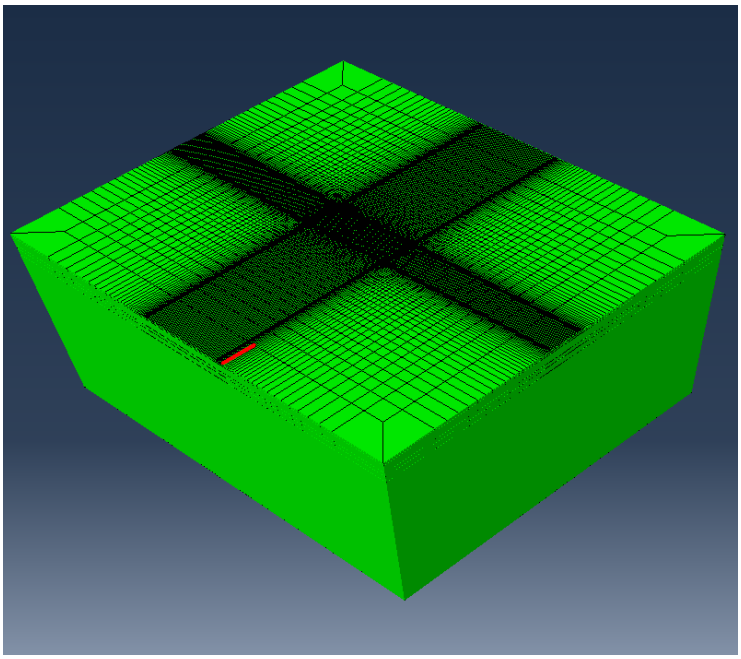

Figure 2: 3-D finite element model

2.3.2 Loading Conditions

LET assumes uniform static vertical pressures within a circular contact area. On the other hand, the tire applies three-dimensional and non-uniform contact stresses that were experimentally measured along with the realistic contact area. FE method considers these true tire-pavement contact loading. Details about tire contact measurements can be found elsewhere (Hernandez et al., 2013). Figure 3 and Figure 4 illustrate representative sketches for the measured contact areas of DTA and NG-WBT, showing clearly that tire footprint may not be simulated as a circular area, although the error may be less in the case of DTA. In addition to the non-uniform contact stress, simulating the tire as a continuous moving load rather than a static steady load is another important realistic consideration in the developed model.

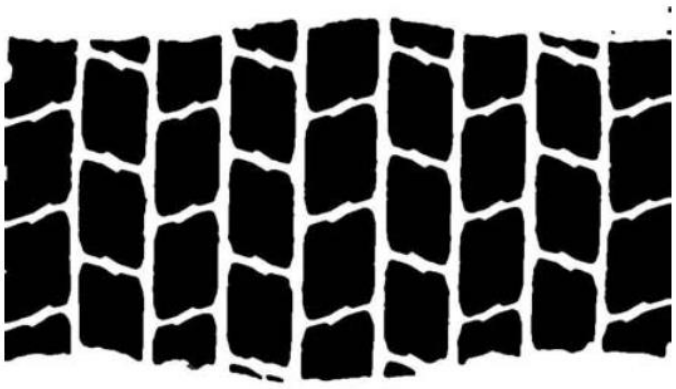

Figure 3:NG-WBT Contact Area (Al-Qadi et al., 2005).

Figure 4: DTA Contact Area (Al-Qadi et al., 2005).

2.3.3 Material Characterization

Asphalt concrete was modelled as a linear viscoelastic material in the developed FE model. ABAQUS characterizes linear viscoelastic material by Prony coefficients obtained from the asphalt concrete master curve. Shear and relaxation moduli are then computed by assuming a constant Poisson's ratio and Prony coefficients. Bulk and shear moduli equations used in ABAQUS are given in Equations 1 and 2. Wlliams-Landell-Ferry function is also used to model time-temperature superposition of AC. (Equation 3).

$$G(t) = G_0\left[1 - \sum_{i=1}^{n} G_i\left(1 - e^{-\frac{t}{\tau_i}}\right)\right] \quad (1)$$

$$K(t) = K_0\left[1 - \sum_{i=1}^{n} K_i\left(1 - e^{-\frac{t}{\tau_i}}\right)\right] \quad (2)$$

where:

G = Shear Modulus

K = Bulk Modulus

t = Reduced Relaxation Time

G_0 and K_0 = Instantenous shear and volumetric modulus

G_i, K_i and τ_i = Prony series parameters

In addition:

$$\log(\alpha_t) = \frac{-C_1(T - T_r)}{C_2 + (T - T_r)} \quad (3)$$

where:

α_t = Shift factor

C_1, C_2 = Regression coefficients

T = Analysis temperature

T_r = Reference temparature

In conventional pavement analysis approaches, both base and subgrade materials are characterized as linear elastic material. However, it has been clearly shown in the literature that the base material exhibits non-linear stress-dependent anisotropic behavior. While non-linearity significantly affects the pavement responses for thin pavement, its effect is negligible for thick pavements where stress levels in base materials are low as tire load is mostly distributed by the relatively thick AC layer. Therefore, in order to reduce computation cost, the base material was modelled as non-linear stress-dependent cross-anisotropic material only for thin pavements. MEPDG model (ARA, 2004) was used to characterize non-linear stress dependent cross-anisotropic behavior of the base materials (Eqs. 4-6).

$$M_{rv} = k_1 \left(\frac{\theta}{p_o}\right)^{k_2} \left(\frac{\sigma_d}{p_o}\right)^{k_3} \quad 4$$

$$M_{rh} = k_4 \left(\frac{\theta}{p_o}\right)^{k_5} \left(\frac{\sigma_d}{p_o}\right)^{k_6} \quad 5$$

$$M_{rs} = k_7 \left(\frac{\theta}{p_o}\right)^{k_8} \left(\frac{\sigma_d}{p_o}\right)^{k_9} \quad 6$$

where:

$M_{rv,} M_{rh}$, M_{rs} = Vertical, horizontal and shear resilient modulus

$\theta = \sigma_1 + \sigma_2 + \sigma_3$ = Bulk stresses

σ_d= deviatoric stress

p_o = Unit reference pressure

k_1, k_2, k_3, $k_{4,} k_5$, k_6, $k_{7,} k_8$, k_9 = Regression coefficients

2.3.4 Analysis Method

There are three commonly used methods for pavement analysis: static, quasi-static, and dynamic analysis. Static analysis assumes that the tire is not moving while it can consider viscoelasticity in the analysis. Quasi-static analysis can model the tire as a moving load; however, it does not capture

the inertial and damping effects. Therefore, dynamic analysis was used in this study to properly simulate moving tire loads with viscoelastic and non-linear material characterization. The dynamic equation solved in ABAQUS is given in Eq. 7. This equation can be solved using the implicit or explicit direct integration method. In this study, the implicit direct integration method was selected because it is more accurate for the level of frequencies observed in pavement simulations.

$$[M]\{\ddot{U}\} + [C]\{\dot{U}\} + [K]\{U\} = \{P\} \quad (7)$$

where:

$[M]$ = Mass matrix

$[C]$ = Damping matrix

$[K]$ = Stiffness matrix

$\{P\}$ = External force vector

{Ü} = Acceleration vector

$\{U\}$ = Displacement vector

2.3.5 Interface Method

The model used for defining how two pavement layers interact with each other is another key parameter for pavement simulation. All AC layers were assumed to be fully bonded to each other in the developed model. On the other hand, AC-base and base-subgrade interaction were simulated using a Coulomb model. In this model, resistance of the movement is assumed to be proportional to the normal stress at the interface. In addition, a tolerance limit was set for shear strength above which two layers start sliding relative to each other in the case of AC-to-base interaction. If relative sliding happens, the frictional stress was assumed to be constant.

2.4 Simulation Matrix Selection

The inputs required for pavement simulations can be mainly divided into three groups: pavement structure (i.e. layer thicknesses and material properties), loading conditions, and material characterization parameters. The value for each of one these inputs parameters can widely differ from one pavement section to another. Hence, it is an impossible task to simulate all possible pavement sections that combines all possible values for each inputs. The study of case selection (i.e. selection of layer thickness, axle loads and tire pressures), therefore, was needed to determine parametric values required for the pavement simulation.

The linear equations were developed based on regression analysis. As a rule of thumb, in order to increase reliability, it is important to stay in the range of inputs of regression based functions. Therefore, it was decided to cover extreme values for each inputs so that extrapolation would be avoided during the implementation of those equations.

The pavement sections were selected based on the two traffic volume conditions: low-volume and interstate highways. The thicknesses were selected in way that they vary between extreme conditions for these two road types (Table 1) A total of ten different tire loadings were simulated. Axle loads and tire pressures were selected to cover extreme load conditions as well (Table 2).

Table 1: Pavement Structure Factorial

	Low-Volume	Interstate Highway
Wearing Surface	75 and 125 mm*	25 and 62.5 mm
Intermediate	75 and 125 mm*	37.5 and 100 mm
Binder	75 and 125 mm*	62.5 and 250 mm
Granular Base	150 and 600 mm	150 and 600 mm

**Note: Low-volume road cases consider only one AC layer*

Table 2: Selected Tire Loading Cases

Tire Type	Axle Load (kN)	Tire Pressure (kPa)
NG-WBT	26.7	552
NG-WBT	26.7	862
NG-WBT	79.9	552
NG-WBT	79.9	862
NG-WBT	44.4	758
DTA	26.7	552
DTA	26.7	862
DTA	79.9	552
DTA	79.9	862
DTA	44.4	758

The Long-Term Pavement Performance (LTTP) database was used to extract material properties for the AC. Approximately 1000 complex modulus data were mined to obtain desired inputs for the pavement simulations. First, nominal maximum aggregate size (NMAS) was decided for each AC layer. While 9.5 - 12.5 mm was selected for NMAS for the wearing surface, 19.5 - 22.5 mm and 25 – 37.5 mm were considered to be typical NMAS for intermediate and binder layer respectively. Afterwards, data was classified into groups based on NMAS for each AC layer and filtered through statistical analysis. Finally, the remaining data was plotted and one strong and one weak complex modulus data were visually chosen for each AC layer.

To select appropriate material parameters for base and subgrade characterization, the database collected by Tutumluer et al. (Tutumluer, 2008) was used. This database has information to determine the k-values in Eqs. 4-6 for 114 different granular materials. Having estimated the stress levels observed in the field from Xiao et al. (Xiao et al., 2011), the resilient modulus of each granular material was calculated at those stress levels. Then mean (μ) and standard deviation (σ) of resilient modulus for all granular materials were computed. Then, weak and strong resilient test data was determined to capture extreme conditions based on high and low stress levels. The lower and upper limits were set as $\mu \pm 2\sigma$. The weak and strong base materials were selected as the ones that have resilient modulus value closer to the lower and upper limits, respectively.

2.5 Results

The objective was to find relationships for converting the pavement response resulting from DTA into NG-WBT. A total of 240 cases were run in ABAQUS for these two different tire types, considering the same material properties and pavement structures. The only difference was the tire-pavement contact, which was measured under the same axle load for NG-WBT and DTA. After plotting the simulation results, the linear relation was observed between the pavement responses of DTA and NG-WBT. Therefore, this relationship is represented as linear functions of DTA. Figure 5 and Figure 6 show the linear equation developed for maximum tensile strain along the traffic and transverse directions at AC surface and bottom of AC. It should be noted that the plots have two different lines: an equality line ($y = x$) and a line of fitted linear function. The equality line is solid while the fitted line is dashed. The purpose of the equality line is to demonstrate the significance of applying an adjustment factor to each particular response.

The linear equations developed a total of 10 different pavement responses. Due to the brevity of the paper, only four plots are presented here. The results for all pavement responses are given in Table 3 with the corresponding coefficients of determination; DTA and NG-WBT refer to pavement responses resulting from these two tire types.

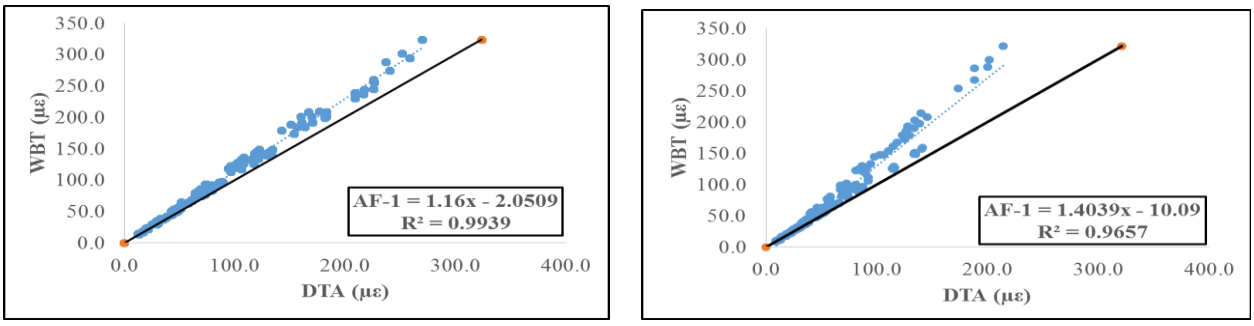

Figure 5: Maximum tensile strain at AC surface in (a) traffic and (b) in transverse directions

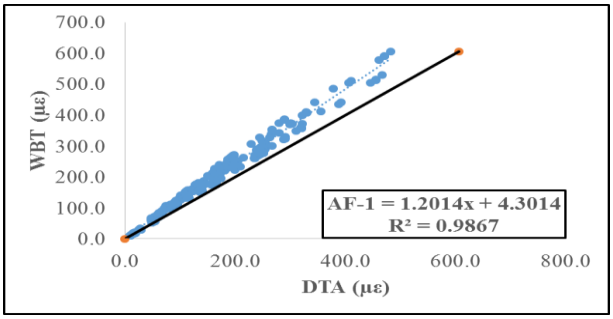

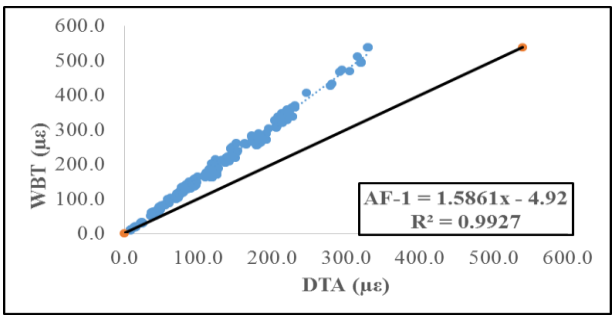

Figure 6: Maximum tensile strain at bottom of AC (a) in traffic and (b) in transverse directions

The linear equations developed a total of 10 different pavement responses. Due to the brevity of the paper, only four plots are presented here. The results for all pavement responses are given in Table 3 with the corresponding coefficients of determination; DTA and NG-WBT refer to pavement responses resulting from these two tire types.

Table 3: Full List of Developed Equations for All Pavement Responses

Pavement Response	Location	Linear Equation	R^2
Maximum Tensile Strain in Traffic Direction	AC Surface	NG-WBT=1.16xDTA-2.05	0.993
Maximum Tensile Strain in Transverse Direction	AC Surface	NG-WBT=1.4039xDTA-10.09	0.965
Maximum Tensile Strain in Traffic Direction	Bottom of AC	NG-WBT=1.20xDTA+4.30	0.986
Maximum Tensile Strain in Transverse Direction	Bottom of AC	NG-WBT=1.59xDTA-4.92	0.992
Maximum Vertical Compressive Strain	Within AC	NG-WBT=1.37xDTA+0.48	0.99
Maximum Vertical Compressive Strain	Within Base	NG-WBT=1.17xDTA+1.23	0.994
Maximum Vertical Compressive Strain	Within Subgrade	NG-WBT=1.16xDTA-4.56	0.989
Maximum Vertical Shear Strain	Within AC	NG-WBT=1.39xDTA-2.85	0.968
Maximum Vertical Shear Strain	Within Base	NG-WBT=1.21xDTA-3.29	0.994
Maximum Vertical Shear Strain	Within Subgrade	NG-WBT=1.11xDTA-0.53	0.99

2.6 Discussion of Results and Main Findings

A total of 480 (240 for DTA, 240 for NG-WBT) simulations were run in ABAQUS to develop a mathematical relationship for pavement responses resulting from these two different tire types. The resulting equation along with the coefficient of determination are given in the previous section. The following are significant observations regarding the effect of NG-WBT tires on pavement responses:

- The coefficients of the DTA variables (i.e., pavement response caused by DTA loading) in the equations are always higher than 1 for all responses. This indicates that NG-WBT causes higher responses than DTA for the same axle load and tire inflation pressure, which might result in greater pavement damage.

- The linear equations were developed for all cases without dividing the cases into subgroups. This means that these linear equations could be applied to DTA responses for predicting NG-WBT response regardless of the material property (weak/strong AC or base characterization) and pavement structure (i.e., thick or thin pavement).
- The fact that the coefficient of determination for all pavement responses is high – between 0.97 to 0.99 – shows that these equations can be implemented to predict NG-WBT loading for mechanistic pavement design guides, like MEPDG, where NG-WBT loading cannot be simulated.
- The value of the coefficient of determination increases as depth of the pavement responses increases because the vertical contact stress becomes the governing factor on pavement responses as the effects of longitudinal and transvers contact stresses diminish.
- The aforementioned observation excludes the maximum tensile strain in traffic direction at AC surface with the coefficient of the determination of 0.99. This exception is attributed to the location of the maximum tensile strain which, although occurs at AC surface, is observed approximately 0.5 m away from the tire where in-plane non-uniform contact stresses lose its effect on the pavement response.
- The most significant difference between NG-WBT and DTA loading was observed on the maximum tensile strain in transverse direction at the bottom of AC. NG-WBT produces approximately 60% higher response than DTA.
- The lowest coefficient of determination was observed for the maximum vertical shear strain within AC, because it is the pavement response most affected by 3-D non-uniform tire contact stress distribution as it occurs approximately 25-75 mm below the surface and in close proximity of the tire-pavement contact.

2.7 Summary

Linear elastic theory (LET) is the pavement analysis method used in MEPDG. NG-WBT loading cannot be simulated in MEPDG because of the unrealistic assumptions and simplifications in implementing LET. Additionally, advance structural techniques like FE analysis are computationally expensive to be used in MEPDG. The study presented in this chapter suggests linear equations to quantitatively define the relationship between pavement responses under DTA and NG-WBT loading. Finite element analysis that is capable of simulating pavement-tire interaction more realistically in terms of material characterization and loading conditions was used to compute pavement responses. A total of 480 cases (240 for DTA and 240 for NG-WBT) that aim to capture extreme values for layer thickness, material characterization parameters, and load conditions were run in ABAQUS. Simulations for DTA and NG-WBT were run considering the same pavement structure and material properties. The only difference was the applied contact loads that were measured for NG-WBT and DTA under the same axle load and tire pressure. It should be noted that validation of the developed equations is part of another study. Results of NG-WBT

and DTA responses at accelerated pavement tests will be used for validation of the introduced equations.

The equations developed show that NG-WBT produces higher responses than DTA for all ten critical pavement responses, which indicates higher damage to pavement. The highest effect of NG-WBT was the maximum tensile strain in transverse direction at bottom of AC. On the other hand, the lowest effect of NG-WBT was observed for the maximum vertical shear strain within subgrade. Higher coefficient of determination values were observed when the axle load governed pavement behavior at increased pavement depths.

The developed equations create an opportunity for MEPDG to consider NG-WBT loading without the requirement of computationally expensive pavement analysis methods. It is recognized that implementation of these equations in MEPDG may require recalibration of the transfer functions used in MEPDG. The traffic composition and the number of axles per truck that uses NG-WBT should also be considered in the pavement analysis, in addition to the fact that NG-WBT market penetration in the US is approximately 10%. Furthermore, the use of NG-WBT should be evaluated in the comprehensive context of pavement-related, economic, and environmental impacts.

CHAPTER 3

COMPARISON OF *MEPDG* PAVEMENT ANALYSIS WITH THE FINITE ELEMENT METHOD

The *Mechanistic-Empirical Pavement Design Guide (MEPDG)* provides theoretically superior methodology, as compared to its predecessor, for design and analysis of pavement structures. The "mechanistic" part refers to simulating pavement–tire interaction to calculate critical responses within pavement. The "empirical" part means prediction of pavement distress propagation over time using transfer functions that link a critical pavement response to a particular pavement distress. The mechanistic part of MEPDG simulates pavement–tire interaction in three steps: subdivision of the pavement layers; complex modulus calculation at the mid-depth of each sublayer, considering velocity and temperature; and running a multilayered elastic theory (MLET) software, JULEA. Although MEDPG has a grounded methodology for pavement analysis, it has a number of limitations and unrealistic simplifications that result in inaccurate response predictions. These limitations are related to the pavement analysis approach used in MEPDG's framework, multilayered elastic theory (MLET). By contrast, finite element (FE) analysis has proven to be a promising numerical approach for overcoming these limitations and simulating pavement more accurately and realistically. Although some other studies compare MLET with FE analysis, none quantifies the difference in pavement response obtained from MEPDG and FE simulations. This study, presented in this chapter, fills that gap by developing linear equations that connect pavement responses produced by these two approaches to pavement analysis. The equations are developed for ten different responses, using a total of 336 cases simulated using FE and MEPDG analyses. The cases modelled in simulations were selected so as to capture extreme conditions, i.e., thick and thin pavement structures with strong and weak material properties. The equations developed can help pavement researchers understand quantitatively the effect of MEPDG's limitations. In addition, the equations may be used as adjustment factors for MEPDG to compute pavement responses more realistically requiring computationally expensive approaches such as FE analysis.

3.1 Introduction

All American Association of State Highway and Transportation Officials (AASHTO) pavement design guides issued between the early 1960s and 1993 are based on empirical equations that rely heavily on the results of the AASHO road test conducted in Ottawa, Illinois, in the late 1950s (AASHTO, 2008). For empirical design guides to deliver accurate performance predictions, design inputs for new pavement structures should be similar to the ones used in the AASHO road test. However, tire type, truck type, axle load limits, and materials have significantly changed since the AASHO road test.

In 1986, researchers, engineers, and transportation institutions clearly recognized the need to have a pavement design guide that incorporates changes in materials and loadings and that considers direct climate effects on pavement performance (AASHTO, 2008). Consequently, NCHRP Project 1-37A was launched in 1998 under the sponsorship of the AASHTO, NCHRP, and FHWA for the development of an advanced and comprehensive design guide. The *MEPDG* was released in 2004. After that, *MEPDG* was reviewed and revised under NCHRP 1-40A, 1-40B, and 1-40D, which resulted in the development of *MEDPG* design software in 2007 (later known as DARWin-ME) and *MEPDG—A Manual of Practice, Interim Edition,* in 2008. In August 2013, the current software version, AASHTOWare Pavement ME Design (AASHTOWare Pavement, N.d.) was released.

In *MEPDG,* the user assumes a pavement structure as a trial design and provides all other inputs to the software, such as traffic, material properties, and environmental conditions. Structural responses (strain, stress, and/or deflections) are then calculated within the pavement, an example of the mechanistic part of the guide. By exploiting empirical models, these responses are linked to distress propagations over a design period and are consequently used for international roughness index (IRI) assessment. Finally, the user checks the design criteria against predicted ones. If design requirements are not satisfied, the trial design should be modified and the steps repeated until they are met. Figure 7 illustrates the MEPDG procedure.

Accurate prediction of pavement responses is key for realistic simulation of distress propagation over time. Although MEDPG has a grounded methodology for pavement analysis, it has a number of unrealistic simplifications that result in inaccurate response predictions. Vertical uniform tire

pressure, circular contact area, linear elastic analysis of AC and base materials, and the spring model assumption for the layer interface can be given as examples of limitations in MEPDG. By contrast, FE analysis simulates pavement responses more realistically in terms of loading conditions and material characterization. However, FE analysis is computationally costly to adopt into the *MEPDG* framework.

In this chapter, linear equations that connect pavement responses obtained from MEPDG to FE analysis are developed. These equations can help pavement researchers to understand quantitatively the effect of limitations and simplifications of MEPDG on pavement responses. Additionally, this study provides MEPDG with the opportunity to obtain more realistic pavement responses without having to implement advanced structural analysis methods like FE analysis. The 3-D flexible pavement finite element model development is presented in Chapter 2.

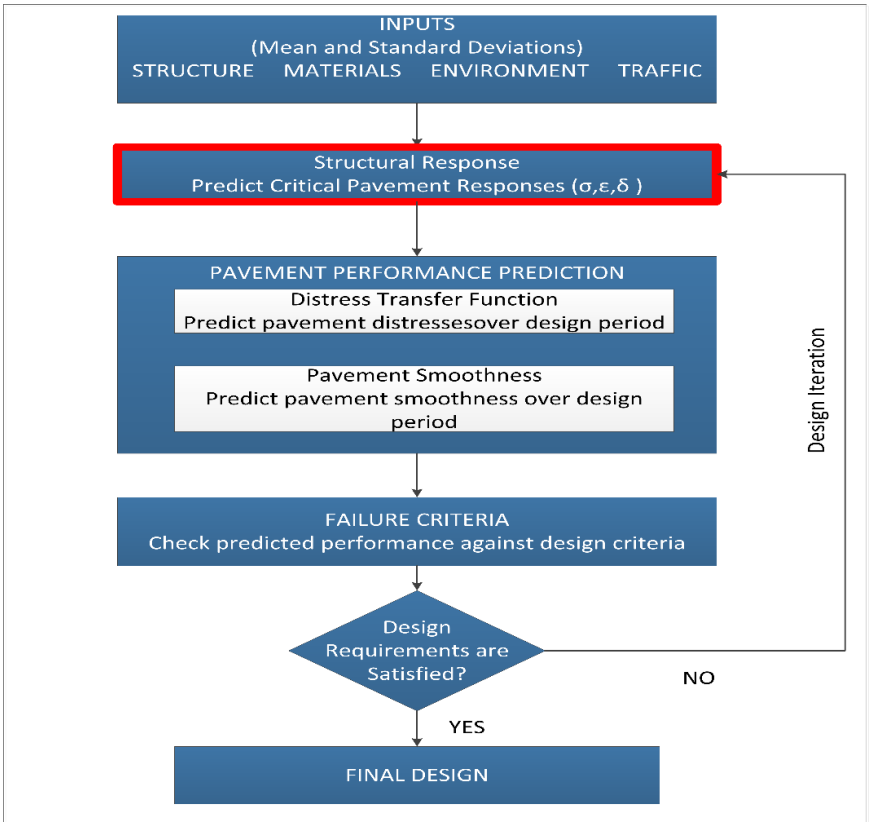

Figure 7: MEPDG flowchart.

3.2 The Mechanistic Part of the MEPDG and Its Limitations

The mechanistic part of the MEPDG refers to pavement analysis conducted for obtaining critical responses. MEPDG exploits the multilayered linear elastic theory (MLET) to compute pavement responses under tire loading. Several types of software implement MLET, such as MnLayer, KenLayer, BISAR, and JULEA; MEPDG uses JULEA in its framework.

MEPDG considers AC as "viscoelastic"; its behavior depends on time, temperature, and frequency of loading. Through a global aging model, MEPDG incorporates the stiffening of the AC layer with time. By contrast, temperature within the pavement is determined using the integrated climate model (ICM). Frequency of loading is calculated as a function of vehicle speed, axle type (single, tandem, or tridem), and pavement structure. In addition, the pavement is divided into sublayers to account for temperature and frequency changes with respect to depth. The dynamic modulus (E^*) is computed at the mid-depth of each sublayer by considering aging, temperature, and frequency and used in JULEA, along with other inputs such as layer thickness, load, and tire pressure.

The mechanistic part consists of a three-step procedure: (1) subdivision of the pavement structure; (2) calculation of the modulus at the mid-depth of each sublayer, considering aging, temperature, and frequency of loading; and (3) running the JULEA with the calculated dynamic modulus and other inputs such as thickness and load. Figure 8 shows the MEDPG procedure for computing pavement responses.

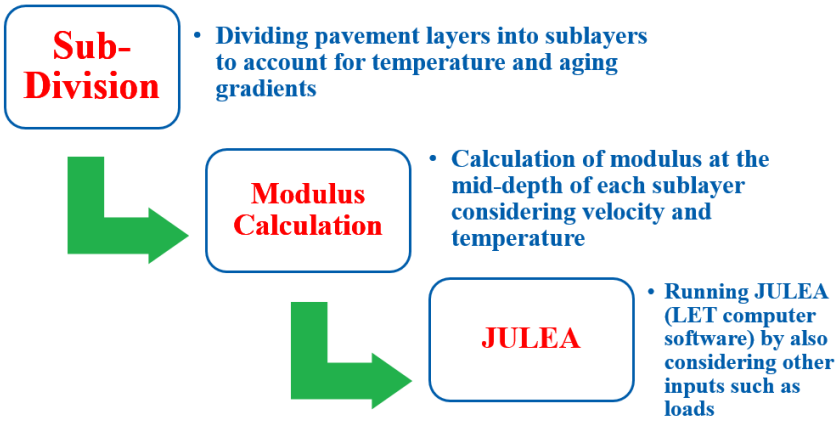

Figure 8: Procedure of MEPDG pavement analysis

Although the mechanistic part of the guide provides a theoretical procedure for computing critical pavement responses, it still has a number of limitations and simplifications, which may lead to unrealistic response prediction. These limitations and simplifications are mostly caused by the assumptions behind the MLET used in MEPDG's framework. By contrast, the FE method can simulate tire–pavement interaction more realistically, thereby overcoming most of MEPDG's limitations.

3.3 Limitations of MEPDG Pavement Analysis

Table 4 demonstrates the limitations of MEPDG by comparing it with FEA (finite element analysis). Tire–pavement interaction is simulated unrealistically because of the assumptions behind the MLET, such as uniform, 2-D vertical tire pressure and a circular contact area.

Table 4: Limitations of the MEPDG Procedure by Comparing It with FE Analysis (FEA)

	FEA	**MEPDG Analysis**
Analysis Type	Dynamic analysis, considering motion of the tire and viscoelasticity of the AC	Linear elastic analysis
Tire Type	Both Wide-Base Tire (WBT) and Dual Tire Assembly (DTA) can be simulated.	Only DTA can be considered.
Contact Stress	Nonuniform, realistically measured, 3-D contact stresses	2-D uniform vertical pressure
Contact Area	True measured tire contact area	Circular contact area
Speed and Temperature	Directly considered in viscoelastic dynamic analysis	Implicitly considered in dynamic modulus calculations
Friction between Layers	Elastic stick model, defined by τ_{max} and d_{max}	Distributed spring model
AC Layer Material Properties	Viscoelastic characterization using Prony series	Dynamic modulus obtained from master curve (*MEPDG* procedure)
Base Layer	Stress-dependent, nonlinear model for base—especially important for thin pavement	Linear elastic

In addition to the limitations given in Table 4, Al-Qadi and coworkers (Al-Qadi et al., 2008a; 2008b) proved that additional errors are introduced by the *MEPDG* procedure for calculating loading frequency, which translates into inaccurate dynamic modulus calculation. MEPDG calculates loading frequency using Equation 8. Al-Qadi et al. (2008b) proved that this conversion does not realistically simulate loading frequency and is thus the first source of error. In the same study, a novel approach is suggested, based on fast Fourier transformation and validated by FE simulations.

$$f = \frac{1}{t} \qquad 8$$

where: t = time of loading(s) and f = frequency of loading (Hz).

Time of loading is calculated as follows:

$$t = \frac{L_{eff}}{17.6\, v_s} \qquad 9$$

where: v_s = vehicle speed, L_{eff} = Effective length.

To calculate effective length, all layer thicknesses are transformed into their equivalent thicknesses based on the stiffness of the subgrade layer. This process is known as Odemark's method of thickness equivalency (Figure 9).

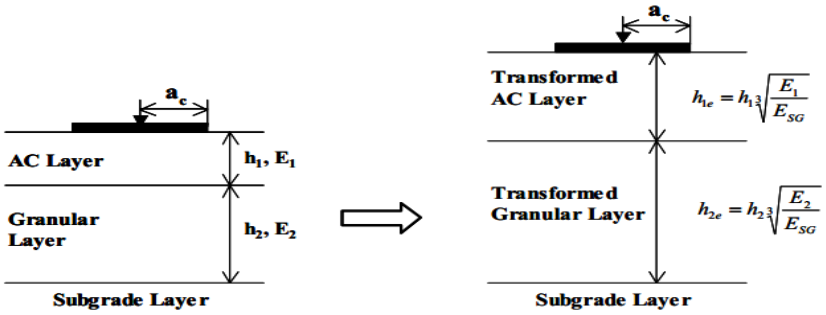

Figure 9: Odemark's method of thickness equivalency (NCHRP, 2004).

After all layer thicknesses are transformed, the effective length (Equation 10) is computed by assuming that stress is distributed at 45° through the soil depth (Figure 10). This assumption is considered the second source of error in frequency calculation. The assumption especially fails to capture the far-field effect of the approaching–leaving rolling wheel (Al-Qadi et al., 2008). The detailed procedure for calculating the frequency of loading is found in NCHRP (2004).

$$L_{eff} = 2 * (a_c + Z_{eff}) \qquad 10$$

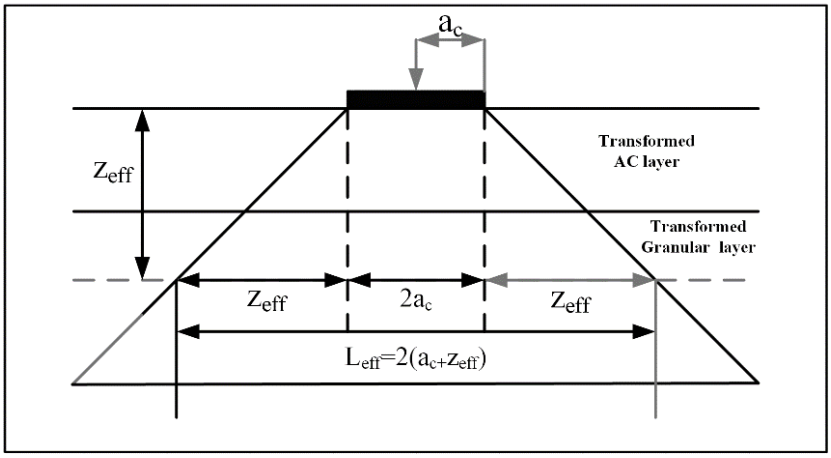

Figure 10: Stress distribution through soil depth.

As explained by Al-Qadi and coworkers (Al-Qadi et al., 2008a; 2008b), the two abovementioned errors may result in a discrepancy up to 140% in loading frequency, depending on vehicle speed and the depth at which calculation is performed.

3.4 Research Methodology

In this chapter, the methodology followed in developing regression-based equations to quantify the relation between MEDPG and FE analysis is explained. The methodology has three main parts: determining the simulations matrix, input conversion from FE analysis to MEPDG, and implementation of the mechanistic part of MEPDG.

3.4.1 Simulation Matrix Selection

Three different inputs are required to conduct pavement analysis: pavement structure (i.e., layer thicknesses), loading parameters, and material characterization parameters. These input parameters can produce values over a very wide range. Hence, an attempt to simulate all possible pavement sections that combines all possible values for each inputs is an impossible task. The study of case selection (i.e., selection of layer thickness, axle loads, and tire pressures), therefore, was needed to determine parametric values required for the pavement simulation.

The linear equations were developed based on regression analysis. As a general rule, to increase reliability, it is important to stay in the range of inputs of the regression-based functions. Therefore, it was decided to cover extreme values for each input so that extrapolation could be avoided during the implementation of those equations.

The selection of pavement structure was based on two extreme conditions: low-volume and interstate highways, which can be interpreted as thin and thick pavement, respectively. The selected thicknesses are given in Table 5. Loading conditions were selected to cover extreme conditions as well (Table 6).

To extract material properties for the AC layer, approximately 1,000 complex modulus data from the long-term pavement performance database were exploit. First, the suitable nominal maximum aggregate size (NMAS) was decided for each AC layer. While 9.5 to 12.5 mm sizes were selected as the NMAS for the wearing surface, 19.5 to 25.0 mm and 25.0 to 37.5 mm were considered to be typical NMAS for the intermediate and binder layers, respectively. Then, the data were classified based on NMAS and filtered through statistical analysis. Finally, the remaining data were plotted, and one strong and one weak complex modulus data were visually chosen for each AC layer.

The database collected by Tutumluer et al. (2008) was used to select appropriate granular material parameters for the base and subgrade layers. First, the estimated stress levels were obtained from Xiao et al. (2011) to calculate the resilient modulus of each material in the database. Afterwards, the mean (μ) and standard deviation (σ) of the resilient modulus for all granular materials were computed. Finally, weak and strong resilient test data were determined, to capture extreme conditions based on high and low stress levels. The lower and upper limits were set as $\mu \pm 2\sigma$.

The base materials selected as weak and strong were the ones that have resilient modulus values closer to the lower and upper limits, respectively.

Table 5: Pavement Structure Factorial

	Low-Volume	Interstate Highway
Wearing Surface	75 and 125 mm*	25 and 62.5 mm
Intermediate	75 and 125 mm*	37.5 and 100 mm
Binder	75 and 125 mm*	62.5 and 250 mm
Granular Base	150 and 600 mm	150 and 600 mm

**Note: Low-volume road cases consider only one AC layer.*

Table 6: Selected Tire Loading Cases

Tire Type	Axle Load (kN)	Tire Pressure (kPa)
DTA	26.7	552
DTA	26.7	862
DTA	79.9	552
DTA	79.9	862
DTA	44.4	758
DTA	26.7	552/758
DTA	79.9	552/758

3.4.2 Input Conversion from FE Model to *MEPDG*

It is critical to convert all inputs used in the FE analysis into the *MEPDG* procedure to be able to run comparable cases.

Table 7 compares all inputs from FEA with those of the *MEPDG* procedure.

Table 7: FEA and MEPDG Input Comparison

	FEA (Reference)	***MEPDG* Procedure**
Axle Load (P)	Not applicable because contact stress are used in FEA	The axle load applied in contact stress experiment
Contact Stress (p)	Nonuniform, 3-D stresses (pressure + traction) measured for each known axle load	2-D uniform vertical stresses—applied inflation pressure in the experiment
Contact Area (A)	True contact area measured for each axle load	Circular (P/p)
Motion of Tire (Speed)	Tire is moved at a given velocity.	Implicitly considered in dynamic modulus calculations
Temperature	Directly considered in viscoelastic analysis	Implicitly considered in dynamic modulus calculations
Friction between Layers	Elastic stick model, defined by τ_{max} and d_{max}	Friction coefficient (user input)
AC-Layer Material Properties	Viscoelastic	Dynamic modulus obtained from master curve
Base Layer	Thick = Elastic modulus	Elastic modulus
	Thin = Stress-dependent nonlinear model	
Subgrade	Elastic modulus	Elastic modulus

The same axle load and tire inflation pressure, applied during experiments to measure contact stresses, were used as loading inputs for *MEPDG*. The contact area was calculated by dividing the axle load by the tire pressure. While speed was used to calculate frequency of loading using Equation 9, the temperature was embedded into the shift factor calculation. The same material

parameters (e.g., elastic modulus and master curve) were given as input in both the FE model and *MEPDG*.

Converting the input parameters used in FE analysis into *MEPDG* form was not complicated except for the pavement interface model parameters. In FE analysis, interaction between layers is simulated by a model called the elastic stick model (ESM). The ESM is an improved version of the well-known Coulomb friction model, presented in Equation 11:

$$\mu = \frac{\tau_{max}}{\sigma} \qquad 11$$

where: μ= Friction coefficient;

$\tau_{\max}$ = Maximum shear stress; and

σ = Normal stress at the interface.

The improvement supplied by the ESM is that it allows tangential stress and a certain amount of elastic slip before the surfaces defining the interface start to slip, as contrasted to the Coulomb model (Figure 11). In Romanoschi and Metcalf (2001), τ_{max} and d_{max} are suggested as 1.415 MPa and 1.6 mm, respectively, for pavement modeling, based on direct shear test results.

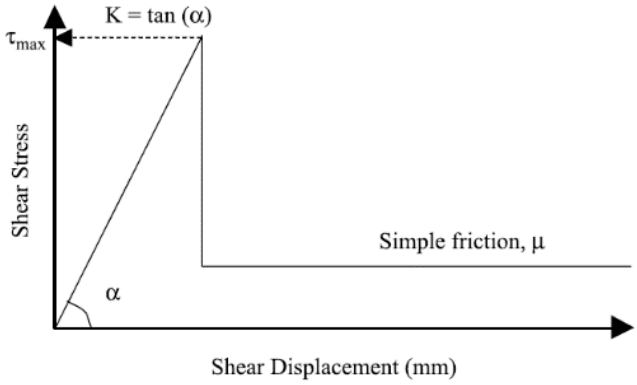

Figure 11: Elastic stick model (Yoo et al., 2006).

By contrast, *MEPDG* assumes uniformly distributed shear spring to connect the interfaces and allow relative horizontal movement between two layers. The spring works in the radial direction and follows the relationship in Equation 12:

$$\tau_i = k_i * (u_i - u_{i+1}) \quad 12$$

where: τ_i= radial shear stress at the interface between layers *i* and *i*+1;

$u_i - u_{i+1}$= relative radial displacement across the interface; and

k_i= interface spring stiffness

To reduce numerical complications, *MEPDG* converts Equation 12 to Equation 13 by using the variable *l* given in Equation 14:

$$(1 - l_i) \cdot \tau_i = l_i \cdot (u_i - u_{i+1}) \quad 13$$

$$k_i = \frac{l_i}{1 - l_i} \quad 14$$

The variable *l* is computed using the user-defined parameter *m*:

$$l = \begin{cases} 0 & \text{for } m \geq 100{,}000 \\ 10^{-m/\mathrm{E}_2} & \text{for } m < 100{,}000 \end{cases} \quad 15$$

where, E_2= Modulus of layer 2 (below the surface layer).

The spring stiffness is basically the slope of τ/d (Figure 11), i.e., ratio of τ_{max} and d_{max}. After spring stiffness is calculated, the user parameter *m* is calculated using Equation 15.

3.4.3 Implementation of the Mechanistic Part of *MEPDG*

Initially, the AASHTOWare software was considered to obtain responses for 336 cases. However, the implementation of the *MEPDG* procedure as a separate numerical tool was needed for two

reasons. First, it is time-consuming and cumbersome to run the AASHTOWare software for 336 cases because the software uses a significant amount of inputs that make comparison to FE results impossible. For instance, the software uses axle load spectra; however, only one set of contact stresses for the specific axle load/tire pressure combination is considered in each FE simulation. In addition, AASHTOWare has temperature-based models for material characterization of the base and subgrade. Conversely, in FE analysis, the base and subgrade are temperature independent, as it would take tremendous effort and time to adopt ICM into the FE model. Second and more importantly, the AASHTOWare software gives only critical pavement responses (e.g., tensile strain at the bottom of the AC or compressive strain within the base layer). Comparing shear strain within the pavement is of interest in this study; however, it is not provided as an output in the software. It is believed that shear strain in AC is relevant to near-surface cracking (Yoo et al., 2008).

Therefore, the *MEPDG* analysis was implemented by using the computer languages MATLAB and AutoHotkey. The main steps to implementing the *MEPDG* procedure are listed below:

1. Subdivision of the pavement structure in sublayers.
2. Calculation of the dynamic modulus at the mid-depth of each sublayer.
3. Creation of the input file.
4. Running JULEA (the linear elastic computer program used by *MEPDG*).
5. Postprocessing to obtain pavement responses.

The pavement subdivision and complex modulus calculation were implemented by following corresponding guidance in *MEPDG*.

3.5 Results

The objective was to identify a relationship for converting the pavement responses resulting from FE analysis into *MEPDG*. A total of 336 cases was simulated by *MEPDG* analysis and FE analysis, using compatible input parameters. Because wide-base tires cannot be simulated in *MEPDG*, loading cases were selected only as dual-tire assembly. To reduce computational time, when implementing AASHTOWare Pavement ME Design software, simplified equations were considered. After plotting the simulation results, the relationship obtained from the two approaches to pavement analysis can be represented by linear equations. However, differences in loading conditions (three-dimensionality and nonuniformity of the contact stresses), material characterization, and layer interaction between FE analysis and *MEPDG* introduce serious

challenges that complicate the development of linear equations. Therefore, in order to obtain statistically acceptable correlations, the cases were divided into three groups: thick pavement, thin pavement with strong base material, and thin pavement with weak base material.

Figure 12 show the linear equations developed for maximum tensile strain along the traffic and transverse directions at the surface and bottom of the AC. The plots show two lines: an equality line ($y = x$) and a line of fitted linear function. The equality line is solid, and the fitted line is dashed. The purpose of the equality line is to demonstrate the significance of applying an adjustment factor to each particular response.

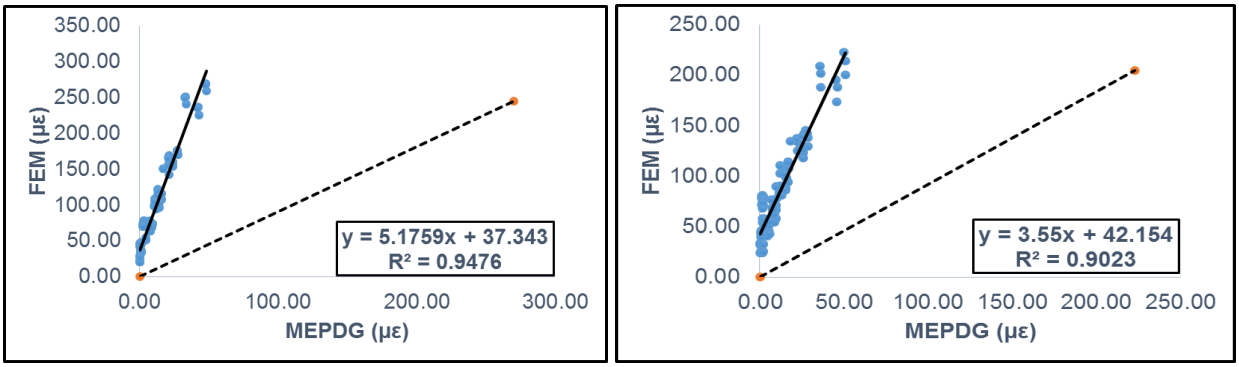

Figure 12: Maximum tensile strain at AC surface in (a) traffic and (b) transverse directions for thick pavement.

The linear equations were developed for ten different pavement responses; two plots are presented herein. The results for all pavement responses are presented in Tables 8 through 11, with the corresponding coefficients of determination.

Table 8: Prediction of FEA parameters from MEPDG results for Thick Pavements

Response	Location	Linear Equation	R2
Maximum Tensile Strain in Traffic Direction	AC Surface	4.63xMEPDG+37.57	0.933
Maximum Tensile Strain in Transverse Direction	AC Surface	3.55xMEPDG+42.15	0.902
Maximum Tensile Strain in Traffic Direction	Bottom of AC	0.85xMEPDG+0.05	0.982
Maximum Tensile Strain in Transverse Direction	Bottom of AC	0.99xMEPDG-2.94	0.969
Maximum Vertical Compressive Strain	Within AC	0.95xMEPDG-9.46	0.969
Maximum Vertical Compressive Strain	Within Base	0.65xMEPDG-6.69	0.947
Maximum Vertical Compressive Strain	Within Subgrade	0.74xMEPDG-10.16	0.981
Maximum Vertical Shear Strain	Within AC	0.55xMEPDG+3.21	0.324
Maximum Vertical Shear Strain	Within Base	0.57xMEPDG-7.03	0.929
Maximum Vertical Shear Strain	Within Subgrade	0.52xMEPDG+10.71	0.954

Table 9: Prediction of FEA parameters from MEPDG results for Thin Pavement with Weak Base

Response	Location	Linear Equation	R2
Maximum Tensile Strain in Traffic Direction	AC Surface	1.71xMEPDG+8.69	0.743
Maximum Tensile Strain in Transverse Direction	AC Surface	1.16xMEPDG+5.88	0.891
Maximum Tensile Strain in Traffic Direction	Bottom of AC	1.23xMEPDG+11.49	0.835
Maximum Tensile Strain in Transverse Direction	Bottom of AC	1.34xMEPDG+12.54	0.739
Maximum Vertical Compressive Strain	Within AC	1.22xMEPDG+5.30	0.919
Maximum Vertical Compressive Strain	Within Base	2.23xMEPDG+140.1	0.918
Maximum Vertical Compressive Strain	Within Subgrade	0.81xMEPDG+10.52	0.836
Maximum Vertical Shear Strain	Within AC	0.38xMEPDG+21.17	0.323
Maximum Vertical Shear Strain	Within Base	1.06xMEPDG+6.37	0.864
Maximum Vertical Shear Strain	Within Subgrade	0.52xMEPDG+45.37	0.581

Table 10: Prediction of FEA parameters from MEPDG results for Thin Pavement with Strong Base

Response	Location	Linear Equation	R2
Maximum Tensile Strain in Traffic Direction	AC Surface	2.51xMEPDG+10.64	0.607
Maximum Tensile Strain in Transverse Direction	AC Surface	1.57xMEPDG+6.54	0.797
Maximum Tensile Strain in Traffic Direction	Bottom of AC	0.93xMEPDG+8.08	0.93
Maximum Tensile Strain in Transverse Direction	Bottom of AC	1.09xMEPDG+2.44	0.87
Maximum Vertical Compressive Strain	Within AC	1.52xMEPDG+7.93	0.849
Maximum Vertical Compressive Strain	Within Base	3.64xMEPDG+118.59	0.894
Maximum Vertical Compressive Strain	Within Subgrade	0.80xMEPDG+101.53	0.725
Maximum Vertical Shear Strain	Within AC	0.37xMEPDG+20.48	0.325
Maximum Vertical Shear Strain	Within Base	1.49xMEPDG+12.78	0.669
Maximum Vertical Shear Strain	Within Subgrade	0.59xMEPDG+56.05	0.556

3.6 Discussion of Results and Main Findings

As discussed earlier, FE and *MEPDG* procedures have significant differences regarding tire–pavement interaction. Among other factors, 3-D nonuniform contact stresses and nonlinear material characterization for the base layer (in the case of thin pavement) seem to result in the highest differences in pavement responses between the two methods. Observations and comments on the results follow.

- After analyses were performed on all cases (*MEPDG* versus FE analysis), two trends were clearly observed based on AC thickness (thick or thin pavement). The effect of contact

stresses diminishes as depth increases. Hence, during the correlation analyses, thin and thick pavements were independently investigated.

- Thin pavements were separated into two groups depending on the base material characterization (i.e., strong or weak) because of its nonlinear, stress-dependent behavior.
- Higher $\boldsymbol{R^2}$-values were obtained for thick pavement than for thin pavement because thick pavement responses were less affected by nonuniform contact stresses. Besides, stress-dependent, nonlinear characterization complicates the comparison between FE and *MEPDG* for thin pavement.
- The coefficients of the independent variable in the fitted equations for thick pavement are smaller than 1 for all the responses except tensile strain at the surface. Consequently, *MEPDG* overestimates the other nine pavement responses.
- There is no regular trend for thin pavement in terms of the coefficients of the independent variable in the fitted equations. Although the *MEPDG* procedure yielded higher values for maximum compressive strain within subgrade, FE resulted in higher values for other responses such, as tensile strain at the bottom of the AC and compressive strain within the AC and base layers.
- Finite element analysis provided higher compressive strain within the base than did *MEPDG's* procedure for thin pavement. This observation emphasizes the importance of considering stress-dependent, nonlinear characterization of the base material.
- The maximum shear strain within AC occurs at shallow depths (around 1 in below the AC surface), so it is governed by the nonuniform, 3-D contact stresses, which are not considered in the *MEPDG* procedure. Hence, as shown in Tables 8 to 10, low $\boldsymbol{R^2}$ (between 0.2 and 0.3) was obtained for maximum shear within the AC.
- Maximum tensile strains at the AC surface occurred far away from the loaded area, where the axle load was the dominant factor on pavement responses. Therefore, the $\boldsymbol{R^2}$ value is generally high for maximum tensile strain at the surface.
- The *MEPDG* procedure underestimates the maximum tensile strain at the AC surface for both thin and thick pavement cases, which conforms to the literature.

3.7 Summary

In the last decade, more states have considered adopting the MEPDG for design and rehabilitation of pavement structures. Although MEPDG has a more theoretically grounded methodology for pavement analysis, as compared with traditional pavement design guides (e.g., 1972, 1986, and 1993 AASHTO), it has a number of limitations and unrealistic simplifications that may result in inaccurate response predictions. Finite element analysis is capable of overcoming these limitations and simulating pavement more accurately and realistically; however, it is computationally too expensive to adapt FE in MEPDG's framework. A total of 336 cases were simulated, using both FE analysis and MEPDG analysis. All input parameters used in the FE analysis were converted into MEPDG analysis to perform valid comparisons. In addition, WBT may not be simulated in MEPDG analysis, hence, only DTA loading was considered in the simulations. Linear equations were developed to quantify the effect of the limitations of *MEPDG's* pavement-simulation approach by comparing it with FE analysis.

The developed equations showed that MEPDG fails to capture the effect of nonuniformity and three-dimensionality of contact stresses. The discrepancy becomes significant for pavement responses of vertical shear strain within AC and tensile strain at AC surface, which are considered the cause for near-surface cracking within AC pavement. By contrast, the differences in pavement responses obtained from MEPDG and FE analyses are reduced as the pavement response depth increases because the effect of longitudinal and transverse contact stresses diminish and vertical contact stress becomes the dominant factor in the pavement response. The importance of characterizing granular material as stress-dependent was highlighted. Results clearly showed that linear elastic characterization of granular material results in stiffer pavement behavior.

The use of the developed equations to modify the MEPDG output responses, allows computing pavement responses more realistically without the requirement of using computationally expensive pavement analysis methods. It is recognized that implementation of these equations in MEPDG may require recalibration of the transfer functions used in MEPDG.

CHAPTER 4

SUMMARY, CONCLUSIONS AND FUTURE WORK

4.1 Summary

The Mechanistic-Empirical Pavement Design Guide (MEPDG), released in 2004, was a significantly improved methodology for designing and rehabilitating pavement structure. It provides a better framework than its predecessors, the ASSHTO 1961, 1972, 1986 and 1993 pavement design guides. The mechanistic part of MEPDG (MEPDG Analysis) computes the critical pavement responses. Those computed pavement responses are linked to corresponding distress by the empirical part of the MEPDG.

MEPDG analysis offers a grounded methodology for simulating pavement tire interactions. It recognizes the fact that AC exhibits viscoelastic behavior and implicitly considers the effects of aging, temperature and frequency of loading. However, its limitations and unrealistic simplifications may still lead to inaccurate pavement response calculations. For example, it simulates tire loading as two-dimensional vertical pressure. Further, contact area is represented by a circle whose area is calculated as dividing axle load by tire pressure. While representing contact area in this way is acceptable for DTA loading, it is not valid for WBT loading. Using a distributed spring model to define the interaction between pavement layers, linear elastic analysis of AC and base materials represent other simplifications existing in MEPDG analysis.

Finite Element (FE) analysis, on the other hand, has proven a promising numerical technique capable of overcoming the aforementioned limitations of MEPDG analysis. It can consider realistically measured three-dimensional tire contact stresses and tire footprint. Moreover, it is capable of simulating non-linearity in material characterization—i.e., the viscolelasticity of AC and stress dependency of base material. However, FE analysis is computationally costly to be adapted into the MEPDG framework. Therefore, this study suggests an approach to reduce the resulted errors in predicting pavement responses to tire loading utilizing MEPDG analysis without directly using FE analysis: developing adjustment factors to modify the pavement responses obtained from MEPDG analysis.

Two sets of adjustment factor are introduced. The first set converts DTA response to WBT, which enables MEPDG to consider WBT loading within its framework (adjustment factor 1). For this adjustment factor, a total of 480 cases (240 for DTA and 240 for NG-WBT) were run in ABAQUS considering the same pavement structure and material properties. The only difference was the applied contact loads that were measured for NG-WBT and DTA under the same axle load and tire pressure. The second set of limitations pertain to the pavement simulation complexities that are not considered in MEPDG (adjustment factor 2). In order to develop this adjustment factor, a total of 336 cases were simulated using both FE analysis and MEPDG analysis using compatible input parameters. Only DTA loading was considered in the simulations since MEDPG analysis is incapable of considering WBT loading. The cases modeled in the simulations were selected in a way to capture extreme conditions, i.e., thick and thin pavement structures with strong and weak material properties.

The results of the adjustment factor showed that NG-WBT produces higher responses than DTA for all ten critical pavement responses, which indicates higher levels of damage to pavement. The highest effect of NG-WBT was the maximum tensile strain in transverse direction at the bottom of AC. On the other hand, the lowest effect of NG-WBT was observed for the maximum vertical shear strain within subgrade. On the other hand, the main findings from adjustment factor 2 is that MEPDG fails to capture the effect of non-uniformity and the three dimensionality of contact stress. The discrepancy becomes significant for pavement responses of vertical shear strain within AC and tensile strain at the AC surface, considered the causes of near surface cracking. On the other hand, the pavement responses obtained from MEPDG and FE analysis get closer as the pavement response depth increases, since the effects of longitudinal and transverse contact stresses diminish as vertical contact stress becomes the dominant factor on pavement response.

The developed adjustment factors create an opportunity for MEPDG to consider NG-WBT loading and realistic pavement-tire interaction conditions without the requirement of computationally expensive pavement analysis methods. It is recognized that implementation of these equations in MEPDG may require recalibration of the transfer functions used in MEPDG.

4.2 Conclusions

This study has the following conclusions:

- In general, NG-WBY produces higher pavement responses than DTA; the difference varies from 10% to 60%.
- Adjustment factors were developed to be used with MEPDG results. This allows considering NG-WBT loading and complexities in pavement behavior without requirement of computationally expensive structural analysis approaches such as FE analysis.

4.3 Future Work

Suggested future work is summarized below:

- Adjustment factor 1 (DTA to NG-WBT) using results from accelerated pavement testing considering the effect of NG-WBT may need to be validated.
- Pavement damage caused by DTA and NG- WBT needs to be compared considering realistic NG-WBT market penetration in truck traffic.
- A comprehensive evaluation is needed of NG-WBT in the context of pavement damage, economic value, and environmental impacts.
- More simulations considering various loading conditions, pavement structures, and material parameters may improve the adjustment factor reliability.

REFERENCES

2013 report card for america's infrastructure (2013). Retrieved from http://www.infrastructurereportcard.org

AASHTO (2008). *Mechanistic-Empirical Pavement Design Guide: A Manual of Practice*, American Association of State Highway and Transportation Officials, Washington, DC

AASHTOWare Pavement: For state-of-the-art pavement design (n.d.). American Association of State Highway and Transportation Officials. Retrieved November 30, 2015, from http://www.aashtoware.org/Pavement/Pages/default.aspx.

Akram, T., Scullion, T., Smith, R. E., & Fernando, E. G. (1992). Estimating damage effects of dual versus wide base tires with multidepth deflectometers. *Transportation Research Record*, (1355).

Al-Qadi, I., & Elseifi, M. (2015). New generation of wide-base tires: impact on trucking operations, environment, and pavements. *Transportation Research Record: Journal of the Transportation Research Board*.

Al-Qadi, I. L., Elseifi, M. A., Yoo, P. J., Dessouky, S. H., Gibson, N., Harman, T., and Petros, K. (2008). Accuracy of Current Complex Modulus Selection Procedure from Vehicular Load Pulse: NCHRP project 1-37a mechanistic-empirical pavement design guide. *Transportation Research Record: Journal of the Transportation Research Board*, *2087*(1), 81–90.

Al-Qadi, I. L., Loulizi, A., Elseifi, M., & Lahouar, S. (2004). The Virginia SMART ROAD: the impact of pavement instrumentation on understanding pavement performance (with discussion). *Journal of the Association of Asphalt Paving Technologists*, *73*.

Al-Qadi, I. L., & Wang, H. (2009). Full-depth pavement responses under various tire configurations: accelerated pavement testing and finite element modeling. *Journal of the Association of Asphalt Paving Technologists*, *78*.

Al-Qadi, I., Wang, H., Yoo, P., & Dessouky, S. (2008). Dynamic analysis and in situ validation of perpetual pavement response to vehicular loading.*Transportation Research Record: Journal of the Transportation Research Board*, (2087), 29-39.

Al-Qadi, I. L., Xie, W., and Elseifi, M. A. (2008). Frequency Determination from Vehicular Loading Time Pulse to Predict Appropriate Complex Modulus in MEPDG. *Journal of the Association of Asphalt Paving Technologists, 77*.

Al-Qadi, I. L., Yoo, P. J., Elseifi, M. A., & Janajreh, I. (2005). Effects of tire configurations on pavement damage (With Discussion). *Journal of the Association of Asphalt Paving Technologists, 74*.

Al-Qadi, I. L., & Yoo, P. J. (2007). Effect of Surface Tangential Contact Stresses on Flexible Pavement Response (With Discussion). *Journal of the Association of Asphalt Paving Technologists, 76*.

Ang-Olson, J., & Schroeer, W. (2002). Energy efficiency strategies for freight trucking: potential impact on fuel use and greenhouse gas emissions.*transportation research record: journal of the transportation research board*, (1815), 11-18.

Applied Research Associates, Inc. (ARA). (2004). Development of The 2002 Guide For The Design Of New And Rehabilitated Pavements. *National Cooperative Highway Research Program (NCHRP) Proj. No. 1-37A*, Transportation Research Board, Washington, DC.

Bonaquist, R. (1992). An assessment of the increased damage potential of wide based single tires. In *International Conference on Asphalt Pavements, 7th, 1992, Nottingham, United Kingdom* (Vol. 3).

Elseifi, M. A., Al-Qadi, I. L., & Yoo, P. J. (2006). Viscoelastic modeling and field validation of flexible pavements. *Journal of engineering mechanics,132*(2), 172-178.

Faber, A., & Hahn, W. D. (2000). Effects of wide single tyres and dual tyres-a technical and economic approach-report on cost 334. *Engineering Transactions, 48*(3), 261-272.

Gungor, O.E., Al-Qadi, I., Gamez, A., and Hernandez, J. (In review). In-Situ Validation of Three-Dimensional Pavement Finite Element Models.

Hernandez, J. A., Al-Qadi, I., & De Beer, M. (2013). Impact of Tire Loading and Tire Pressure on Measured 3-D Contact Stresses. *Airfield and Highway Pavement 2013: Sustainable and Efficient Pavements*.

Huhtala, M. (1986, June). The effect of different trucks on road pavements. In *Proc., the International Symposium on Heavy Vehicle Weights and Dimensions*.

Huhtala, M., Pihlajamaki, J., & Pienimaki, M. (1989). Effects of tires and tire pressures on road pavements. *Transportation research record*, (1227).

National Cooperative Highway Research Program (NCHRP) (2004). *Guide for Mechanistic-Empirical Design of New and Rehabilitated Pavement Structures. Final Report for Project 1-37A*, Part I, Chapter I. Washington DC: NCHRP, Transportation Research Board, National Research Council.

Romanoschi, S., and Metcalf, J. (2001). Characterization of asphalt concrete layer interfaces. *Transportation Research Record: Journal of the Transportation Research Board*, 1778, 132–139.

Sebaaly, P., & Tabatabaee, N. (1989). *Effect of tire pressure and type on response of flexible pavement* (No. 1227).

Siddharthan, R. V., Yao, J., & Sebaaly, P. E. (1998). Pavement strain from moving dynamic 3D load distribution. *Journal of Transportation Engineering*,*124*(6), 557-566.

Simulia, D. S. (2013). *Abaqus 6.13 User's Manual.* Dassault Systems, Providence, Rhode Island.

Tutumluer, E. (2008). State of the Art: Anisotropic Characterization of Unbound Aggregate Layers in Flexible Pavements. *Pavements and Materials: Modeling, Testing*, 1-16.

U.S. Greenhouse Gas Inventory Report: 1990:2013 (2014). Retrieved from http://www.epa.gov/climatechange/ghgemissions/usinventoryreport.html

Wang, H., & Al-Qadi, I. (2009). Combined effect of moving wheel loading and three-dimensional contact stresses on perpetual pavement responses.*Transportation Research Record: Journal of the Transportation Research Board*, (2095), 53-61.

Wang, H., & Al-Qadi, I. L. (2010). Impact quantification of wide-base tire loading on secondary road flexible pavements. *Journal of Transportation Engineering*, *137*(9), 630-639.

Xiao, Y., Tutumluer, E., & Siekmeier, J. (2011). Mechanistic-empirical evaluation of aggregate base and granular subbase quality affecting flexible pavement performance in minnesota. *Transportation Research Record: Journal of the Transportation Research Board*, (2227), 97-106.

Yoo, P. J., Al-Qadi, I. L., Elseifi, M. A., & Janajreh, I. (2006). Flexible pavement responses to different loading amplitudes considering layer interface condition and lateral shear forces. *The International Journal of Pavement Engineering*, *7*(1), 73-86.

Yoo, P., & Al-Qadi, I. (2007). Effect of transient dynamic loading on flexible pavements. *Transportation Research Record: Journal of the Transportation Research Board*, (1990), 129-140.

Yoo, P. J., & Al-Qadi, I. L. (2008). The Truth and Myth of Fatigue Cracking Potential in Hot-Mix Asphalt: Numerical Analysis and Validation (With Discussion). *Journal of the Association of Asphalt Paving Technologists*, *77*.

APPENDIX A: Full plots of Adjustment Factor 1 (DTA to NG-WBT)

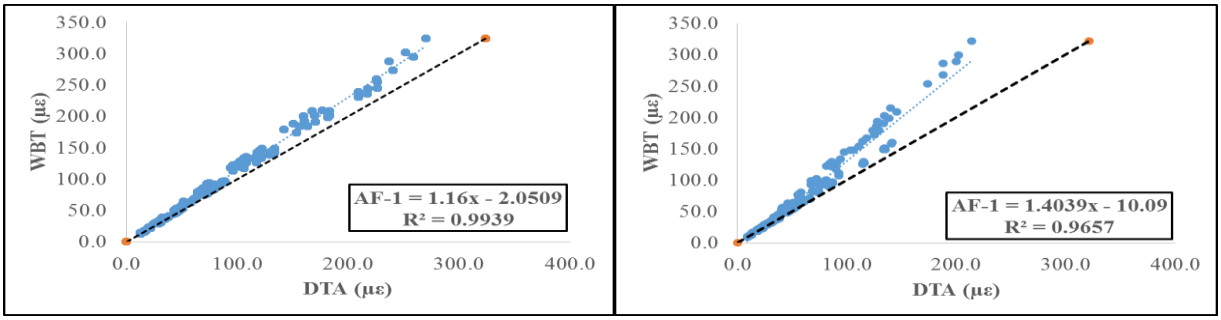

Figure 13: Maximum tensile strain in traffic and transverse direction at AC surface.

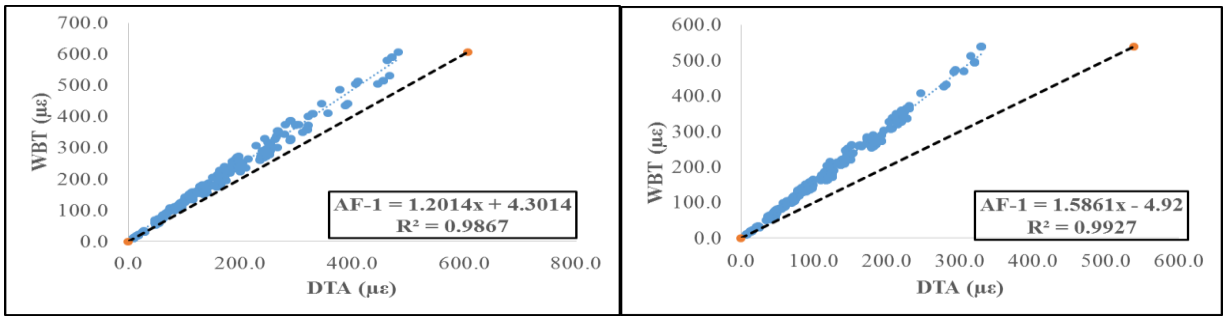

Figure 14: Maximum tensile strain in traffic and transverse direction at bottom of AC.

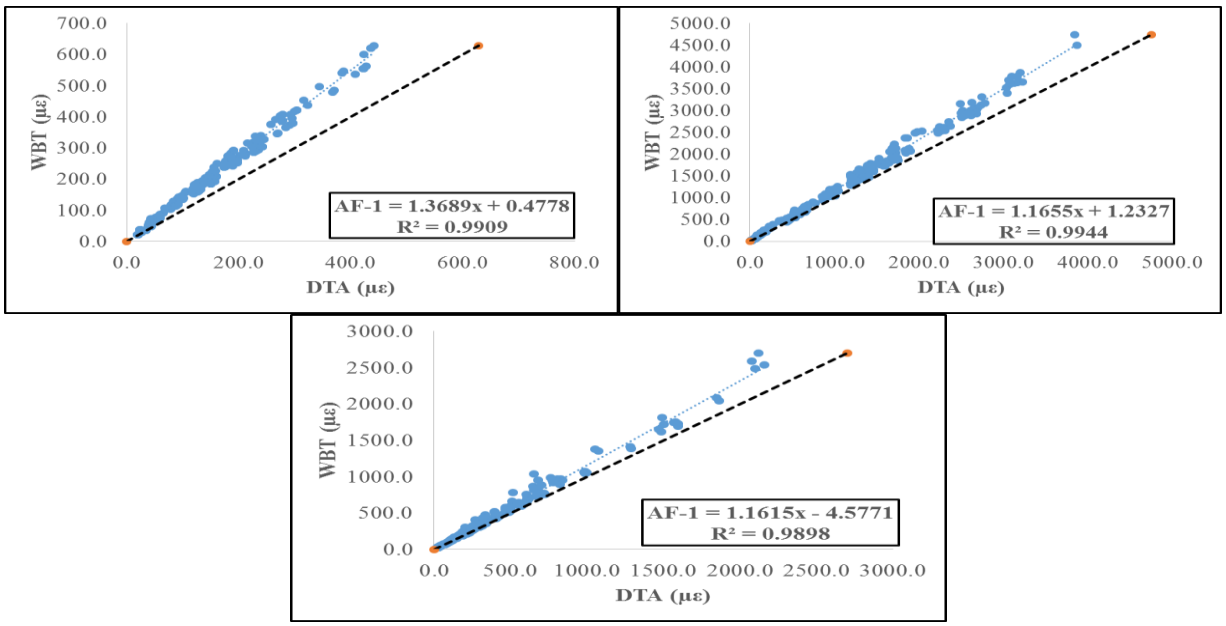

Figure 15: Maximum compressive strain within AC, base, and subgrade.

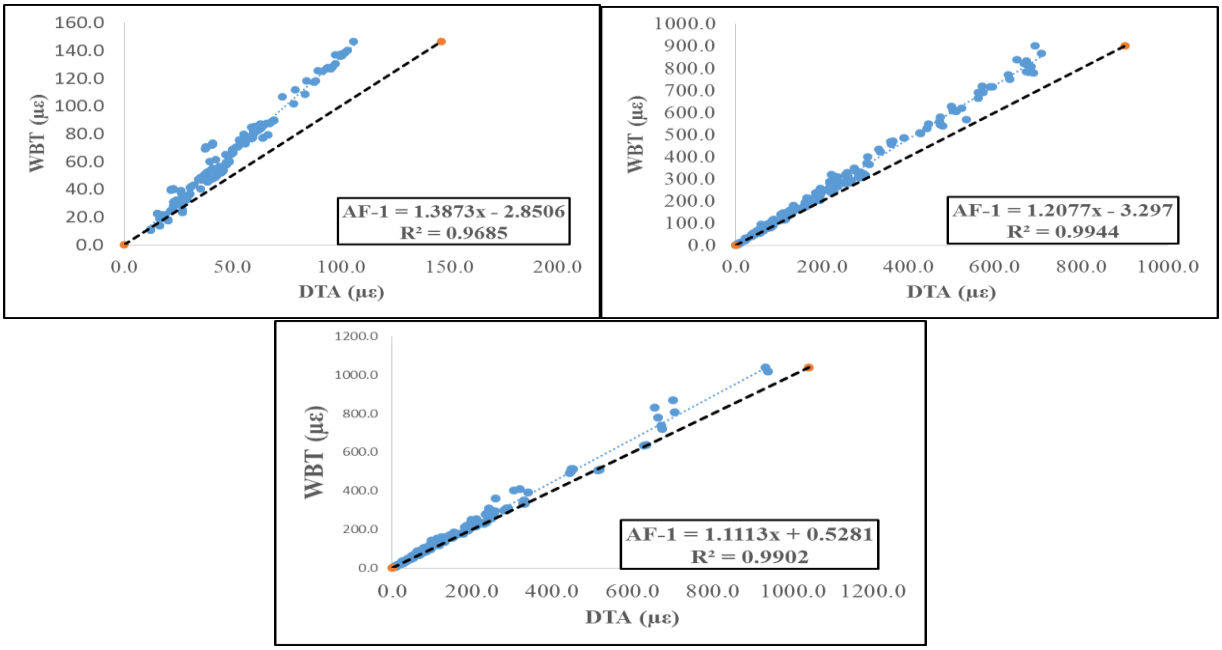

Figure 16: Maximum shear strain within AC, base, and subgrade.

APPENDIX B: Full plots of Adjustment Factor 2 (MEPDG Analysis to FE Analysis)

APPENDIX B.1: Adjustment Factor 2 for Thick Pavement

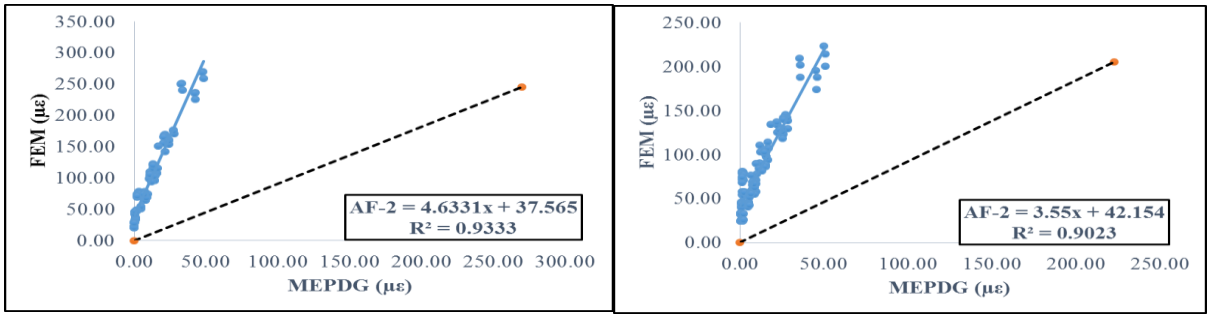

Figure 17: Maximum tensile strain in traffic and transverse direction at AC surface

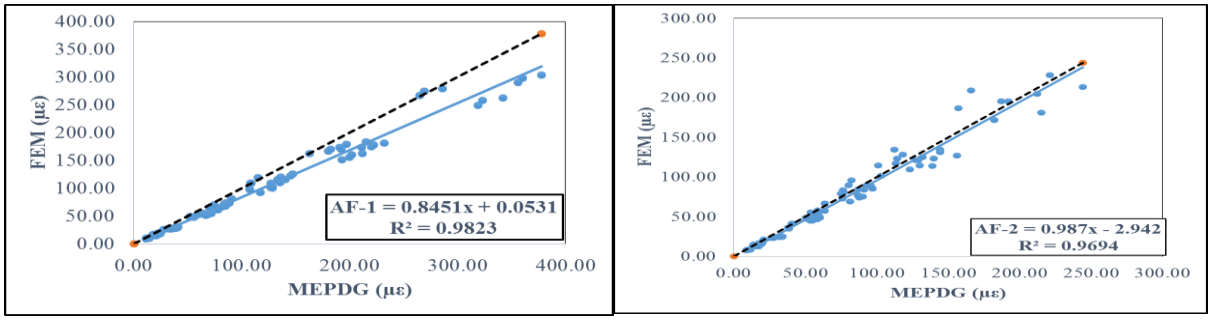

Figure 18: Maximum tensile strain in traffic and transverse direction at bottom of AC

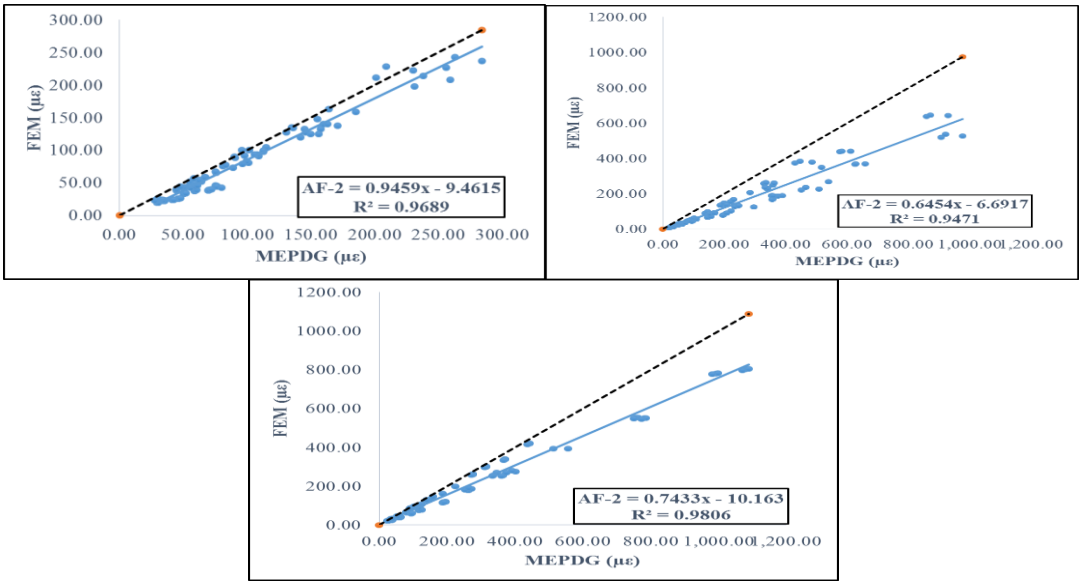

Figure 19: Maximum compressive strain within AC, base, and subgrade

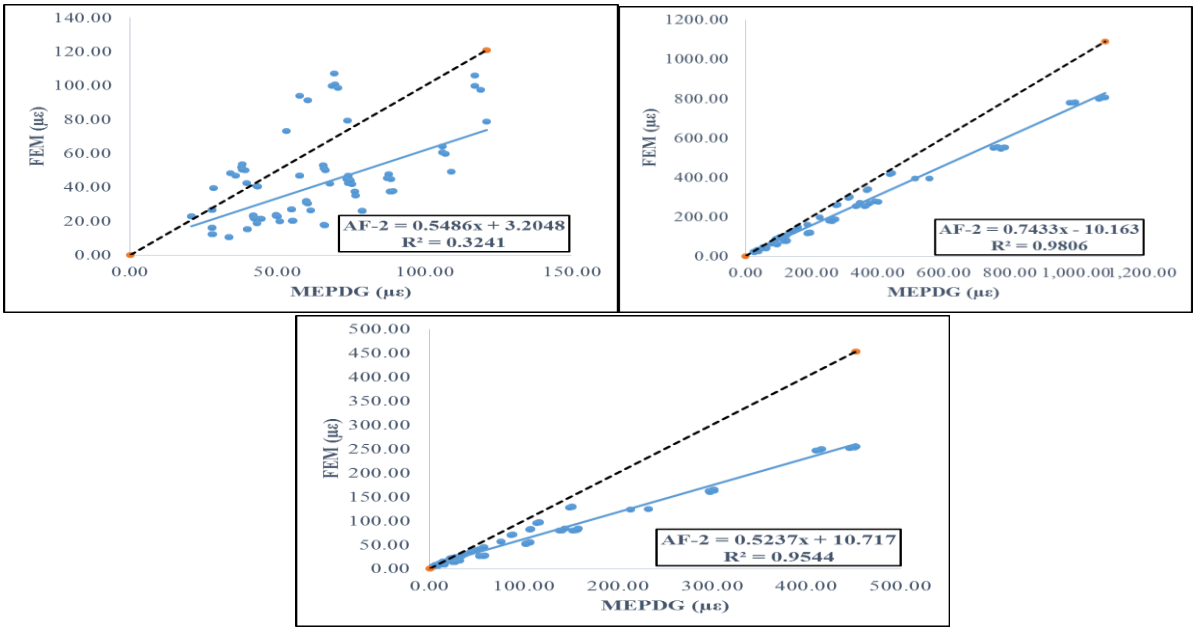

Figure 20: Maximum shear strain within AC, base, and subgrade

APPENDIX B.2: Adjustment Factor 2 for Thin Pavement for Weak and Strong Base

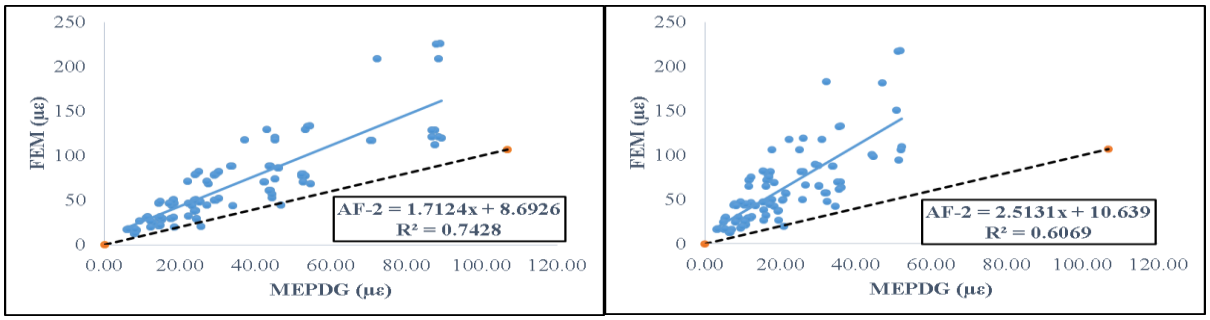

Figure 21: Maximum tensile strain in traffic direction at AC surface for weak and strong base layers

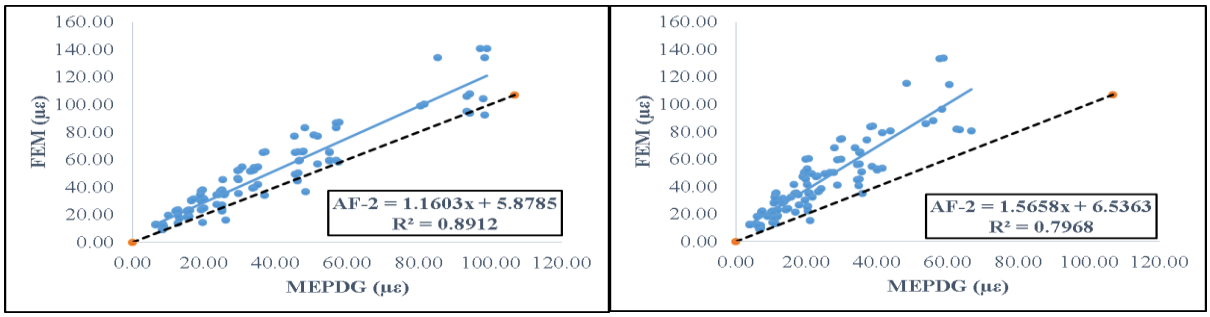

Figure 22: Maximum tensile strain in transverse direction at AC surface for weak and strong base layers

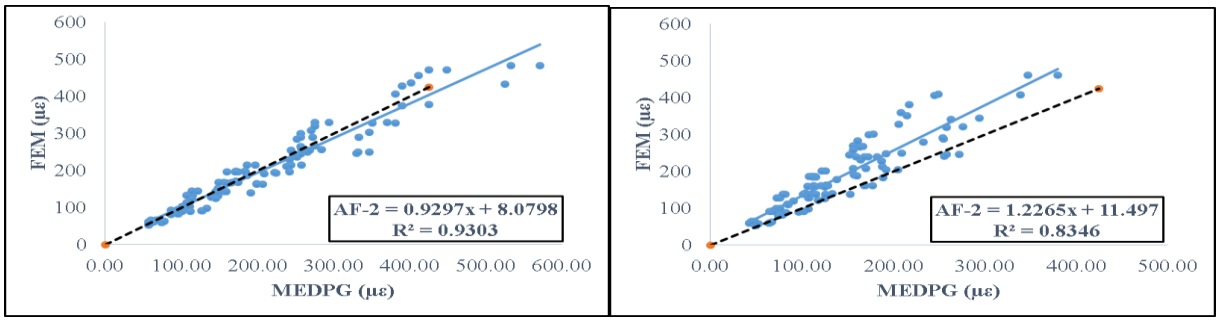

Figure 23: Maximum tensile strain in traffic direction at bottom of AC for weak and strong base layers

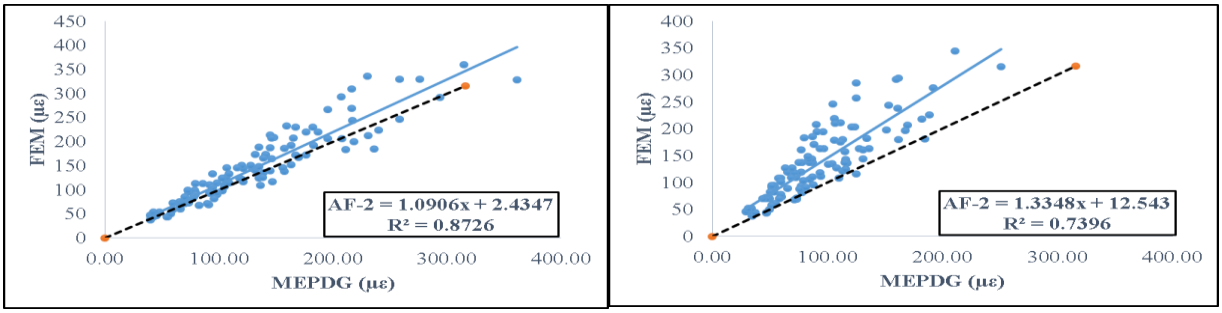

Figure 24: Maximum tensile strain in transverse direction at bottom of AC for weak and strong base layers

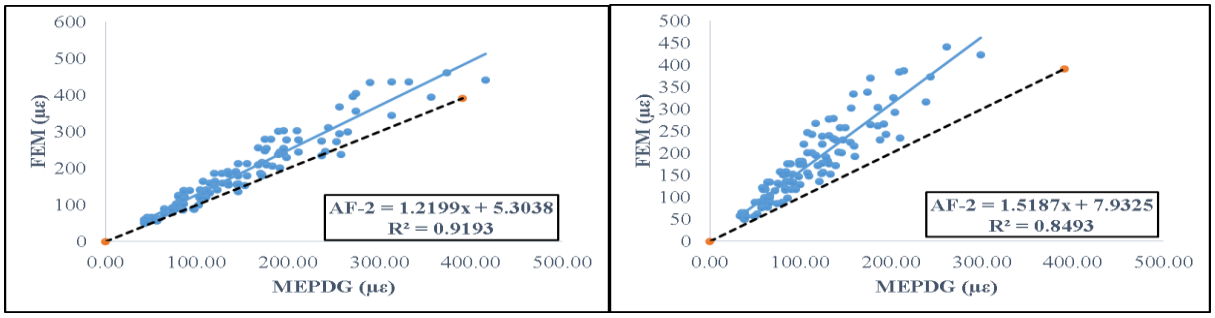

Figure 25: Maximum compressive strain within AC for weak and strong base layers

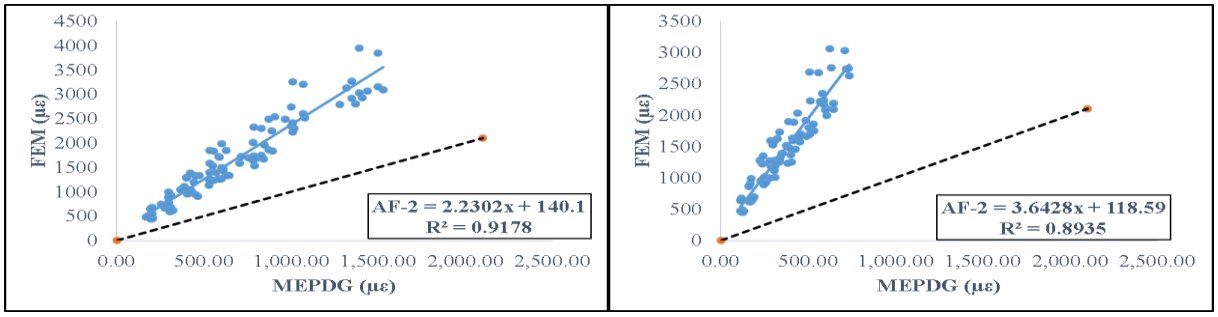

Figure 26: Maximum compressive strain within base for weak and strong base layers

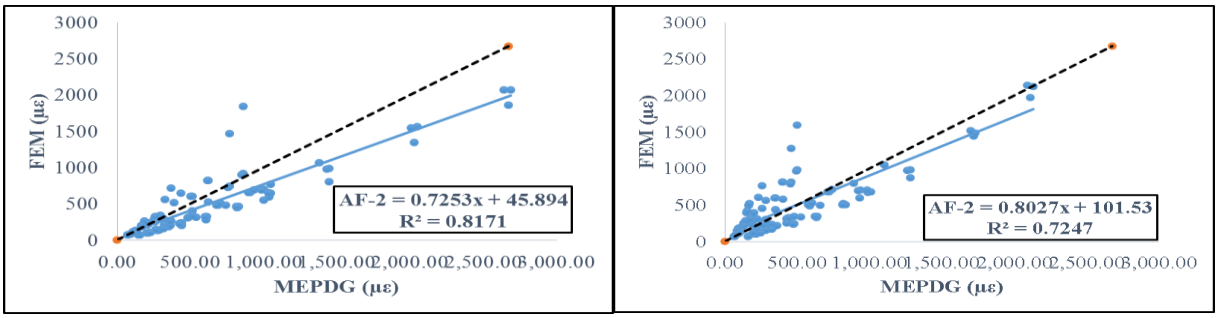

Figure 27: Maximum compressive strain within subgrade for weak and strong base layers

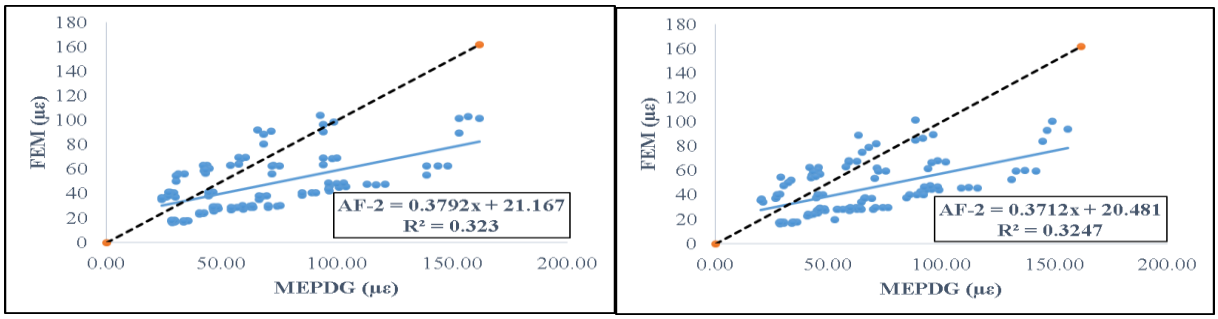

Figure 28: Maximum shear strain within AC for weak and strong base layers

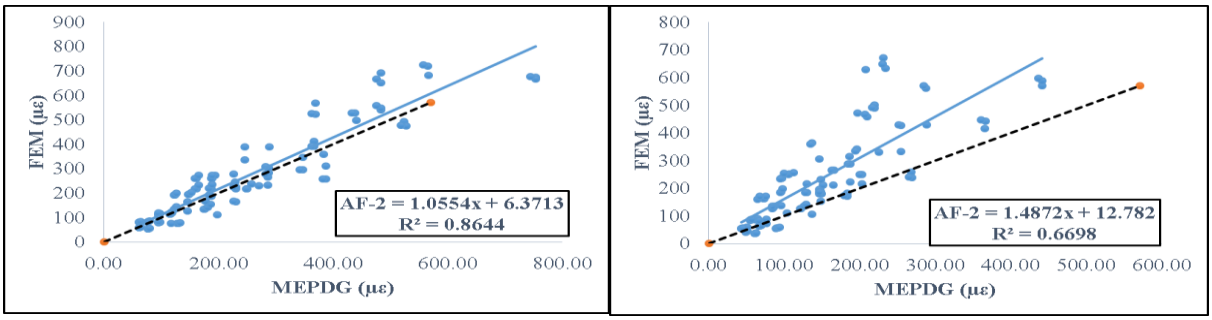

Figure 29: Maximum shear strain within base for weak and strong base layers

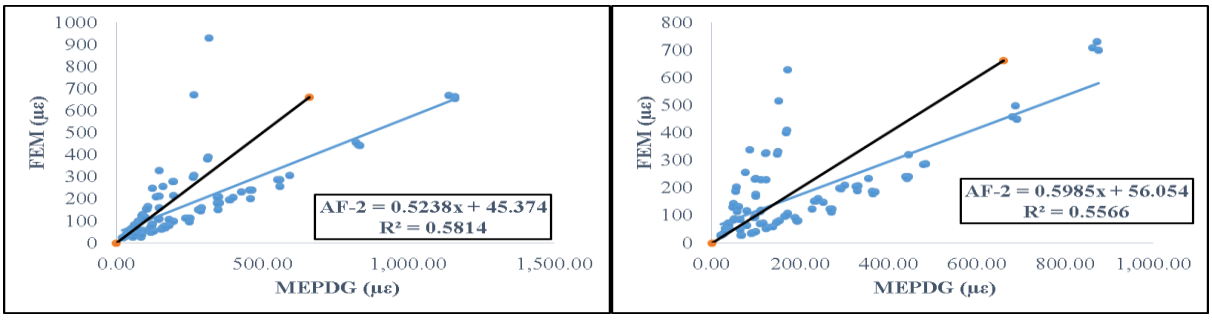

Figure 30: Maximum shear strain within subgrade for weak and strong base layers